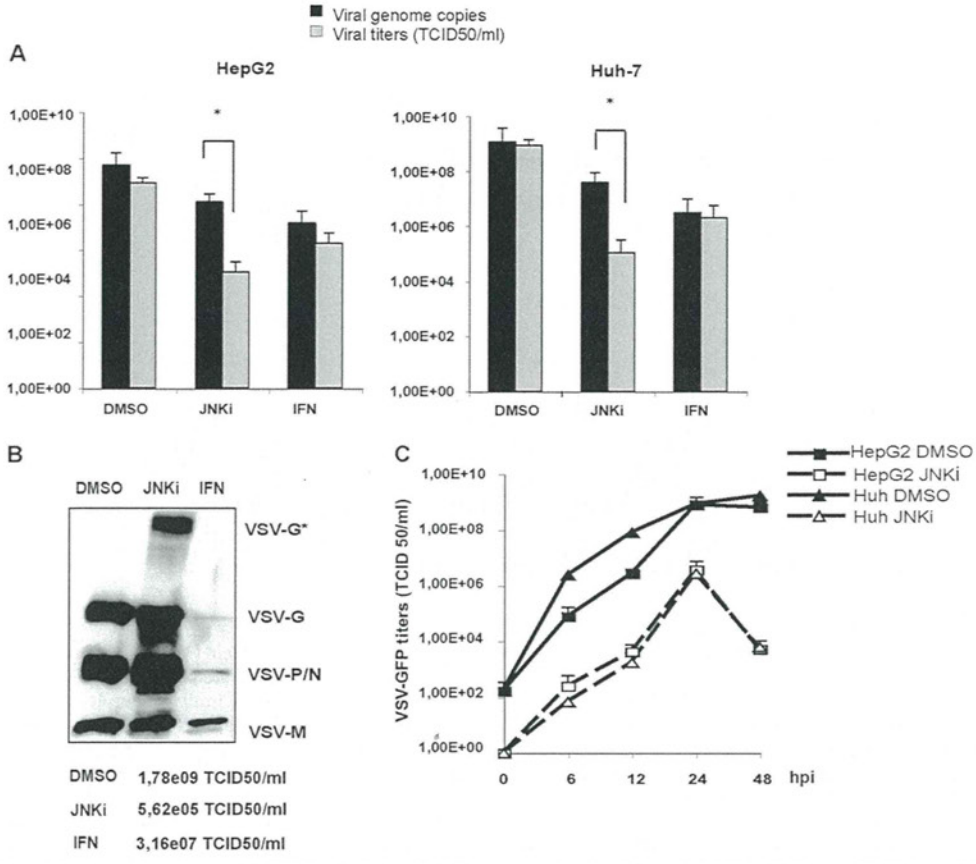

FIG 4 The JNK inhibitor SP600125 interferes with VSV infectivity. (A) Viral titers obtained from DMSO-, SP600125 (JNKi)-, and IFN-treated cells were compared to the corresponding genome copy numbers. Infection was performed for 16 h, and viral genomic RNA in the supernatants was analyzed by real-time PCR, whereas the viral titer was determined by $TCID_{50}$ assay. Upon treatment with SP600125, the difference between viral titers and genome copy numbers was significant (*, $P < 0.05$). (B) Semipurified viruses obtained from DMSO-, SP600125 (JNKi)-, and IFN-treated cell supernatants by ultracentrifugation were used to determine VSV protein expression by Western blotting. Viral titers of the samples shown are listed at the bottom. (C) Determinations of growth kinetics on HCC cells were performed in the presence of vehicle (DMSO) or SP600125 (JNKi). Cells were infected with VSV at an MOI of 0.1, and viral titers were determined by $TCID_{50}$ analysis at the indicated time points. Mean values and standard deviations from triplicate experiments are shown.

the cells were treated either with DMSO or with SP600125. The extent of syncytium formation was quantified at 24 h posttransfection by using a syncytium index (SI) (Fig. 7A, left). Syncytium formation was also visualized in transfected cells not treated (DMSO) or treated with SP600125 (JNKi) by the staining of nuclei with propidium iodide (Fig. 7A, right) The fusion activity of VSV-G in the presence of the JNK inhibitor was significantly reduced. The VSV growth attenuation in HCC cells was proportional to the concentration of SP600125 (Fig. 6B). The decrease in viral titers correlated directly with the level of expression of VSV-G* in infected cells; at a concentration of 25 μM, VSV growth was attenuated by about 10,000- to 100,000-fold, while VSV-G* was maximally expressed (Fig. 6C). Levels of the wild-type VSV G and M proteins remained unchanged.

DISCUSSION

VSV is an oncolytic virus, which selectively grows and kills a variety of cancer cells and shows an attenuated growth phenotype in normal cells. VSV selectivity is achieved by exploiting molecular defects in cancer cells, which compromise the innate antiviral defense or, on the other hand, create advantages for malignant growth and survival (38, 45). The potent cytolytic properties of VSV in conjunction with its rapid replication cycle have made VSV an extremely promising candidate for oncolytic virotherapy (1, 31, 43, 52). Interestingly, many of the signaling pathways that viruses use are the same ones deregulated during malignant evolution. Due to their relevance in oncogenesis, these same pathways have become targets for anticancer drug development. Now that oncolytic viruses are finally entering the clinic, the time has come to take a further step forward and explore possible new application strategies involving the most up-to-date and refined anticancer agents. Therefore, it is reasonable to foresee the great potential of synergistic combinations of oncolytic viruses and small cell-permeable inhibitors of protein kinases to enhance tumor killing. For example, the various MAPK pathways (ERK1/2, JNK, and p38 MAPK) appear to be some of the most significant cellular signaling cascades in the development of several malignancies, including HCC (36, 47, 49). Therefore, the inhibition of ERK can be useful to control the growths of several human cancers (40), while JNK modulators are able to induce cancer cell death or sensitize tumor cells to apoptotic stimuli (12, 41). The JNK pathway has also been linked to cell cycle progression and antiviral responses (3, 13, 22, 42). In addition, the MAPK pathways play an important role in the life cycles of certain viruses (10, 19, 33, 46, 61). In view

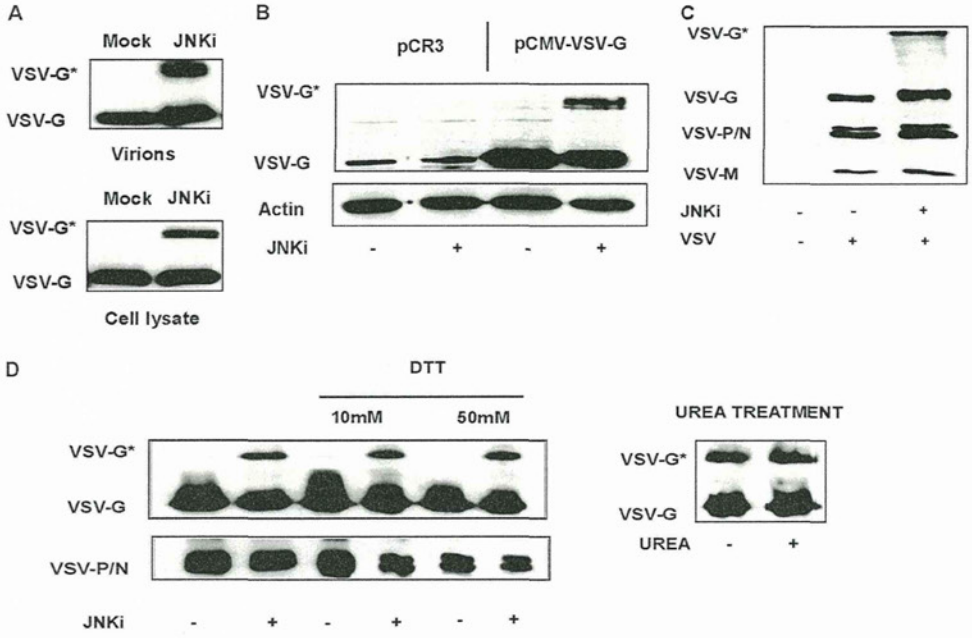

FIG 5 SP600125 induces a posttranslational modification of the VSV-G protein. (A) Levels of viral glycoprotein (VSV-G) from isolated viral particles (top) or infected-cell lysates (bottom) were analyzed by Western blotting. Huh-7 cells, used as representative cells, were pretreated with SP600125 (JNKi) or with the vehicle (DMSO) and infected with VSV at an MOI of 0.1 for 24 h. A fast-migrating band (VSV-G) was identified in all the samples and represents the mature form of the VSV glycoprotein. When infection was performed in the presence of SP600125, a slower-migrating band (VSV-G*) was present. (B) Huh-7 cells were transfected with an empty vector (pCR3) or with a vector expressing the VSV glycoprotein (pCMV-VSV-G). Cells were cultured for 24 h in the presence of DMSO or SP600125 (JNKi), and cell lysates were analyzed by Western blotting using a specific anti-VSV-G antibody. (C) Western blot analysis of VSV obtained from DMSO-treated or SP600125-treated (JNKi) cells. Levels of the VSV glycoprotein (G), phosphoprotein/nucleoprotein (P/N), and matrix protein (M) were detected by an anti-VSV serum (kindly provided by Douglas Lyles). (D) Semipurified VSV obtained from DMSO- or SP600125-treated cultures was subjected to DTT reduction. (Left) Lysates were treated with 10 or 50 mM DTT and loaded together with untreated controls on an SDS-PAGE gel. (Right) The same samples were alternatively exposed to 8 M urea and analyzed by Western blotting.

of a combinatorial approach with new drugs based on the specific targeting of MAPK and oncolytic viruses, we investigated the use of such combinations using VSV in the context of HCC.

In this work, we have studied the influence of three of the major MAPK inhibitors on VSV oncolysis *in vitro*, comparing HCC cell lines with primary human hepatocytes. It was previously shown that ERK facilitates VSV-mediated oncolysis by the negative regulation of the IFN-α response (43). In many HCC cell lines, the innate immunity response to pathogens is compromised, especially due to multiple defects in the type I IFN system (38). The reestablishment of a functional type I IFN response in HCC would be seriously detrimental to the therapeutic efficacy of VSV. Our studies demonstrated that in HCC cell lines, the activation of the ERK signaling pathway does not enhance VSV oncol-

TABLE 1 Identification of SP600125-induced high-molecular-mass VSV-G* by MS

Positions of fragment	Expected mass (kDa)	Measured mass (kDa)	Δ mass	No. of misses	Sequence
1–11	1,357.84	1,357.75	0.09	1	KFTIVFPHNQK
16–44	3,328.6	3,328.56	0.04	0	NVPSNYHYCPSSSDLNWHNDLIGTAIQVK
51–63	1,489.70	1,489.64	0.05	0	AIQADGWMCHASK
84–100	1,996.93	1,996.94	−0.01	1	SFTPSVEQCKESIEQTK
175–200	2,834.21	2,834.30	−0.09	0	GLCDSNLISMDITFFSEDGELSSLGK
207–217	1,235.50	1,235.55	−0.05	0	SNYFAYETGGK
231–249	2,123.14	2,123.05	0.09	1	LPSGVWFEMADKDLFAAAR
250–277	3,033.54	3,033.42	0.12	0	FPECPEGSSISAPSQTSVDVSLIQDVER
278–290	1,641.85	1,641.77	0.08	0	ILDYSLCQETWSK
293–308	1,639.91	1,639.91	−0.01	0	AGLPISPVDLSYLAPK
333–342	1,053.55	1,053.62	−0.07	0	VDIAAPILSR
343–354	1,313.58	1,313.60	−0.01	0	MVGMISGTTTER
355–375	2,472.19	2,472.16	0.04	0	ELWDDWAPYEDVEIGPNGVLR
382–401	2,292.10	292.09	0.01	0	FPLYMIGHGMLDSDLHLSSK
402–432	3,398.62	3,398.61	0.01	0	AQVFEHPHIQDAASQLPDDESLFFGDTGLSK
433–446	1,690.87	1,690.84	0.03	0	NPIELVEGWFSSWK
483–492	1,297.53	1,297.60	−0.07	0	QIYTDIEMNR

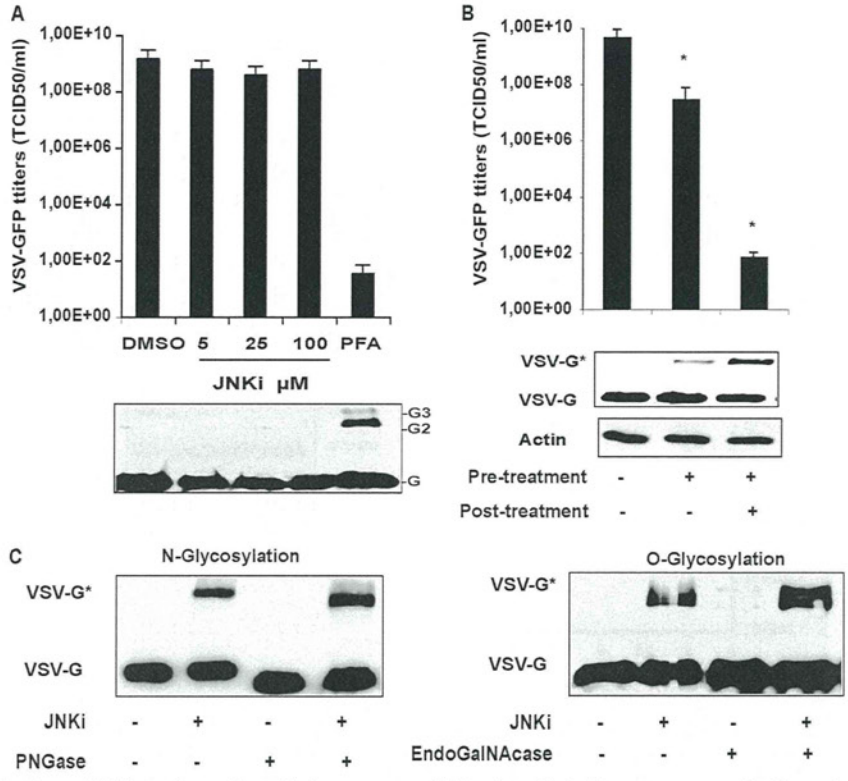

FIG 6 VSV-G* is not the result of cross-linking or hyperglycosylation processes. (A) Semipurified virions were exposed to increasing concentrations of SP600125 (JNKi) for 1 h on ice. As a control, virions were cross-linked with PFA (2%) on ice for 15 min. One-tenth of the samples was preheated at 56°C for 10 min and loaded onto an SDS-PAGE gel. Viral glycoprotein monomers (G), dimers (G2), and trimers (G3) were detected with a polyclonal antibody specific for VSV-G (bottom). The same samples were used to infect HepG2 cells, and viral progeny was quantified by $TCID_{50}$ analysis at 24 h postinfection. (B) Huh-7 cells were pretreated with SP600125 and infected with VSV-GFP at an MOI of 1. Infection was carried out without or in the presence of the inhibitor SP600125 for 24 h. DMSO-treated cells were used as a control. Viral titers and levels of VSV-G and VSV-G* in the corresponding cell lysates are shown and represent the means of data from three independent experiments. (C) Semipurified virions obtained in the presence or absence of SP600125 were digested with PNGase F (left) or EndoGalNAcase (right) overnight. After digestion, the expression levels of VSV-G and VSV-G* were analyzed by Western blotting.

ysis, since protection from lytic infection was not improved by the coadministration of the ERK inhibitor U0126 and IFN-α/β. Therefore, the disruption of ERK signaling by anticancer drugs seems to be compatible with VSV therapy in HCC, at least *in vitro*. The discrepancy of our results compared with those of previous reports (43) emphasizes the need to consider each cancer type as a unique environment. For this reason, preliminary *in vitro* studies assume a great significance in view of subsequent clinical investigations.

Since their discovery in the early 1990s, JNKs have attracted intense interest due to the increasing evidence of the involvement of JNK-dependent signaling events in the development of several pathological conditions. The potential therapeutic application of JNK-specific inhibitors for the treatment of different human diseases, from ischemia, diabetes, and cancer to viral infectious diseases, has been explored (25, 34, 39). Notably, JNK1 has an essential oncogenic role in HCC development, and direct evidence comes from *in vivo* studies with JNK1 knockout mice. In mice lacking JNK1, diethylnitrosamine-triggered liver tumorigenesis was remarkably reduced, and treatment with chemical JNK inhibitors resulted in the reduced growth of xenografted human HCC cells (22, 42). Besides SP600125 (3), several small-molecule compounds inhibiting JNK kinase activity with higher selectivity and efficacy have been developed (35), and the combination of these new inhibitors with VSV virotherapy could potentially be beneficial for HCC treatment.

Increasingly, it has been shown that viral infection can lead to stress-activating protein kinase (SAPK)/JNK and p38 MAPK activation, which is needed for viral replication and release (21, 39, 54, 61). In this report, we observed a strong activation of JNK upon the infection of HCC cell lines with VSV, while the levels of activation of ERK and p38 MAPK were very weak. Inhibitors of p38 MAPK (SB203580) and of ERK (U0126) did not reduce the viral yield in HCC cells. On the other hand, the JNK inhibitor SP600125 dramatically decreased viral titers in all cell types tested, consistent with previous studies with dengue virus, rotavirus, and circovirus (7, 19, 56). SP600125 and other similar anthrapyrazoles are considered to be valuable therapeutic agents; their usefulness against cancer (3, 15), liver injury, and fibrosis (20, 29) has been associated with minimal toxicity *in vivo*. Unfortunately, in light of our results, we excluded the possibility of a conjunctive application of SP600125 and VSV therapy. However, our results indicate that the attenuation of VSV by SP600125 is due to a nonspecific mechanism that does not involve the inhibition of JNK, and therefore, the combination of VSV and other specific JNK inhibitors still represents a viable treatment option.

Most interestingly, despite the fact that the numbers of copies of the viral genome in the supernatants of SP600125-treated cells

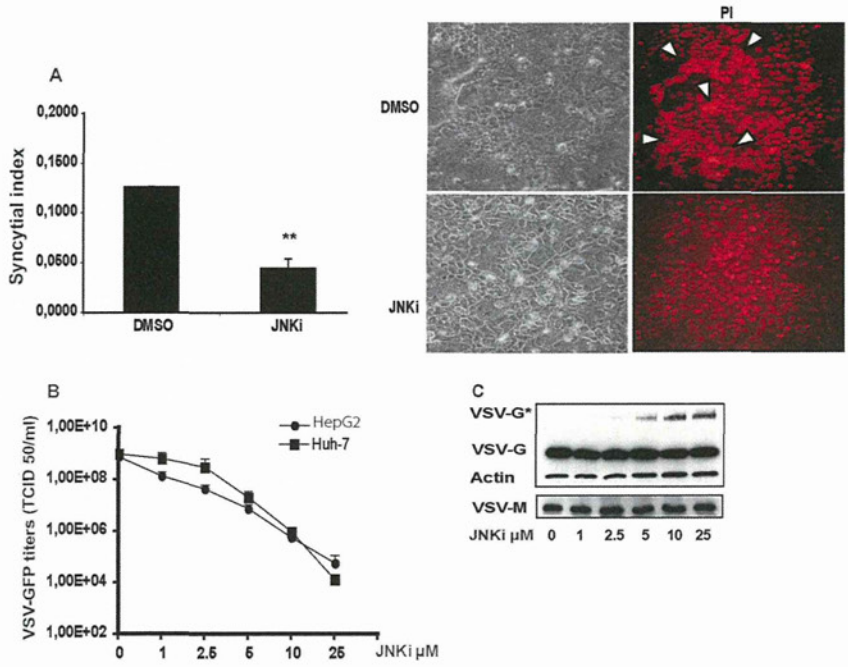

FIG 7 SP600125 decreases the fusion activity of VSV-G. (A) Huh-7 cells were transfected with an expression vector for the VSV glycoprotein (pCMV-VSV-G). At 8 h posttransfection, supernatants were replaced with fresh medium containing either DMSO or SP600125 (25 μM). Syncytium formation was quantified by the determination of the syncytium index (SI) (Fig. 6A, left), and parallel cultures were fixed and stained with propidium iodide (PI) to visualize syncytia (Fig. 6A, right). **, $P < 0.01$. (B) HCC cells were treated with increasing concentrations of SP600125 and infected with VSV at an MOI of 0.1 for 24 h. Aliquots of the supernatants were subjected to $TCID_{50}$ assay for determination of viral titers. Means and standard deviations of data from duplicate experiments are shown. (C) Expression levels of VSV-G and VSV-G* were analyzed by Western blotting in the corresponding cell lysates (data for HepG2 cells are shown as representative data). The maximum expression level of VSV-G* was at 25 μM SP600125, the concentration which corresponds to the greatest attenuation of VSV.

did not differ substantially from those in the untreated controls, the infectious viral titers were significantly lower, up to 10,000- to 100,000-fold. These results led us to conclude that SP600125 affects VSV infectivity such that only a fraction of the new viral progeny released into the culture supernatant retains the ability to reinfect cells. As a cause of a lack of infectivity of newly formed virions, we have found that the viral particles incorporate at least two different forms of the G protein in the presence of SP600125: one that comigrates with the normal G protein and the other that is significantly higher in molecular mass than the normal G protein (VSV-G*). The same result was observed when a VSV-G protein-expressing plasmid was transfected in the presence of the JNK inhibitor.

At this point, we speculated that VSV-G* could represent either a hyperglycosylated form of VSV-G or a VSV-G dimer, since the size was roughly twice the size of the monomeric G protein. An alteration of glycosylation can have a dramatic impact on the infectivity of viruses; as observed previously by Whitt and colleagues, virions incorporating a glycoprotein with an additional N-linked oligosaccharide in the extracellular domain were not infectious, apparently due to the formation of heterodimers that lacked fusion activity (58). In our experiments, digestion with *N*- or *O*-glycosidases did not completely abolish VSV-G* expression, leading us to the conclusion that this form was not assignable to a hyperglycosylated status (Fig. 6C). Intriguingly, VSV-G* may represent a protein complex or an as-yet-unknown modification of the G protein that is thermostable and resistant to SDS; additionally, it does not dissociate under reducing conditions (DTT) and is not denatured by urea. Moreover, exposure to an acidic pH at an elevated temperature did not to affect the detection of VSV-G* (data not shown).

The incubation of extracellular VSV with SP600125 did not lead to VSV-G* formation, nor did it hamper viral infectivity, ruling out a possible cross-linking activity of SP600125. Pretreatment alone with infection carried out in the absence of SP600125 resulted in reduced levels of VSV-G* and a partial recovery of viral titers.

Mass spectrometry analysis revealed that VSV-G* contains only peptides from the VSV G protein. In repeated experiments, we did not identify any cellular protein consistently in VSV-G* preparations, including the ones related to major posttranslational modifications, such as ubiquitination, sumoylation, neddylation, and ISGylation, etc. (23, 27, 50, 55, 59). Despite the fact that we were able to exclude several mechanisms involved in protein modifications, the nature of VSV-G* still remains enigmatic, yet it is possible that unidentified modifications through covalent linkages are responsible for the formation of VSV-G*. Given the difficulty in identifying these processes, further studies will be required to address this important aspect.

The presence of VSV-G* species compromised the fusion activity of the VSV glycoprotein; in the presence of SP600125, the expression of VSV-G* led to a reduction in levels of syncytium formation. Since increased levels of VSV-G* expression depend on the SP600125 concentration and correlate inversely with viral titers, we postulate that SP600115 attenuates VSV by hampering the VSV glycoprotein fusogenic activity.

In conclusion, our *in vitro* results support the concept that combination therapy using oncolytic VSV and MAPK inhibitors

might result in synergistic antitumor activity against HCC, and we plan to test this hypothesis in future *in vivo* studies. Furthermore, at the molecular level, we have provided new insights into the antiviral properties of the inhibitor SP600125. SP600125 also attenuates the growths of several viruses of different families, suggesting a possible common mechanism of action that could be exploited for the development of antiviral treatment. A very intriguing application of SP600125 could be as a treatment of viral infections that are accompanied by malignant transformation. Both antiviral and antitumor effects of the drug could have significant benefits, for example, in the treatment of hepatitis C virus or human papillomavirus infection (16, 60). The elucidation of viral posttranslational control and viral mechanisms of infectivity can also be investigated by means of the effect of SP600125 on VSV-G maturation, leading to the development of new and targeted antiviral strategies.

ACKNOWLEDGMENTS

We are thankful to Barbara Lindner and Stefanie Mühlhans for their excellent technical assistance. We thank Alexander Muik (Georg Speyer Haus, Institute for Biological Research, Frankfurt am Main, Germany) and Dorothee von Laer (University of Innsbruck, Austria) for providing the VSV-G expression vector. The MS analysis was carried out at the Proteomics Core Facility at the University of Nebraska—Lincoln. We are grateful to Douglas Lyles for providing anti-VSV and anti-VSV-M antibodies. We are also thankful to Lilianna Schyschka and Claudine Seeliger for primary human hepatocyte isolation.

This work is supported in part by the German Cancer Aid (Max Eder Research Program), the Federal Ministry of Education and Research (grant 01GU0505), and the SFB 824 (DFG Sonderforschungsbereich 824), German Research Foundation, Bonn, Germany.

S.M., J.A., E.N.D.T., A.K.P., and O.E. conceived of and designed the experiments; S.M., S.A., P.X.D., and A.R. performed the experiments; S.M., P.X.D., and A.K.P. analyzed the data; A.N., N.K., and R.M.S. contributed reagents, materials, and/or analysis tools; and S.M., J.A., A.K.P., and O.E. wrote the paper.

REFERENCES

1. **Altomonte J, et al.** 2008. Synergistic antitumor effects of transarterial viroembolization for multifocal hepatocellular carcinoma in rats. Hepatology **48**:1864–1873.
2. **Banerjee S, et al.** 2008. Hepatitis C virus core protein upregulates serine phosphorylation of insulin receptor substrate-1 and impairs the downstream Akt/protein kinase B signaling pathway for insulin resistance. J. Virol. **82**:2606–2612.
3. **Bennett BL, et al.** 2001. SP600125, an anthrapyrazolone inhibitor of Jun N-terminal kinase. Proc. Natl. Acad. Sci. U. S. A. **98**:13681–13686.
4. **Bode AM, Dong Z.** 2007. The functional contrariety of JNK. Mol. Carcinog. **46**:591–598.
5. **Bogoyevitch MA.** 2006. The isoform-specific functions of the c-Jun N-terminal kinases (JNKs): differences revealed by gene targeting. Bioessays **28**:923–934.
6. **Cargnello M, Roux PP.** 2011. Activation and function of the MAPKs and their substrates, the MAPK-activated protein kinases. Microbiol. Mol. Biol. Rev. **75**:50–83.
7. **Ceballos-Olvera I, Chavez-Salinas S, Medina F, Ludert JE, del Angel RM.** 2010. JNK phosphorylation, induced during dengue virus infection, is important for viral infection and requires the presence of cholesterol. Virology **396**:30–36.
8. **Chen F, Castranova V.** 2009. Beyond apoptosis of JNK1 in liver cancer. Cell Cycle **8**:1145–1147.
9. **Clarke P, et al.** 2004. JNK regulates the release of proapoptotic mitochondrial factors in reovirus-infected cells. J. Virol. **78**:13132–13138.
10. **Clarke P, Meintzer SM, Widmann C, Johnson GL, Tyler KL.** 2001. Reovirus infection activates JNK and the JNK-dependent transcription factor c-Jun. J. Virol. **75**:11275–11283.
11. **Corcoran JA, et al.** 2006. The p14 fusion-associated small transmembrane (FAST) protein effects membrane fusion from a subset of membrane microdomains. J. Biol. Chem. **281**:31778–31789.
12. **Dhanasekaran DN, Reddy EP.** 2008. JNK signaling in apoptosis. Oncogene **27**:6245–6251.
13. **Du L, et al.** 2004. Inhibition of cell proliferation and cell cycle progression by specific inhibition of basal JNK activity: evidence that mitotic Bcl-2 phosphorylation is JNK-independent. J. Biol. Chem. **279**:11957–11966.
14. **Ebert O, et al.** 2003. Oncolytic vesicular stomatitis virus for treatment of orthotopic hepatocellular carcinoma in immune-competent rats. Cancer Res. **63**:3605–3611.
15. **Hanajiri K, et al.** 2009. Echographic detection of diethylnitrosamine-induced liver tumors in rats and the effect of the intratumoral injection of an inhibitor of c-Jun N-terminal kinase. J. Gastroenterol. Hepatol. **24**: 866–871.
16. **Hassan M, Ghozlan H, Abdel-Kader O.** 2005. Activation of c-Jun NH2-terminal kinase (JNK) signaling pathway is essential for the stimulation of hepatitis C virus (HCV) non-structural protein 3 (NS3)-mediated cell growth. Virology **333**:324–336.
17. **Heasley LE, Han SY.** 2006. JNK regulation of oncogenesis. Mol. Cells **21**:167–173.
18. **Hirasawa K, et al.** 2003. Effect of p38 mitogen-activated protein kinase on the replication of encephalomyocarditis virus. J. Virol. **77**:5649–5656.
19. **Holloway G, Coulson BS.** 2006. Rotavirus activates JNK and p38 signaling pathways in intestinal cells, leading to AP-1-driven transcriptional responses and enhanced virus replication. J. Virol. **80**:10624–10633.
20. **Hu YB, Liu XY.** 2009. Protective effects of SP600125 in a diet-induced rat model of non-alcoholic steatohepatitis. Scand. J. Gastroenterol. **44**:1356–1362.
21. **Huerta-Zepeda A, et al.** 2008. Crosstalk between coagulation and inflammation during dengue virus infection. Thromb. Haemost. **99**:936–943.
22. **Hui L, Zatloukal K, Scheuch H, Stepniak E, Wagner EF.** 2008. Proliferation of human HCC cells and chemically induced mouse liver cancers requires JNK1-dependent p21 downregulation. J. Clin. Invest. **118**:3943–3953.
23. **Isaacson MK, Ploegh HL.** 2009. Ubiquitination, ubiquitin-like modifiers, and deubiquitination in viral infection. Cell Host Microbe **18**:559–570.
24. **Iyoda K, et al.** 2003. Involvement of the p38 mitogen-activated protein kinase cascade in hepatocellular carcinoma. Cancer **97**:3017–3026.
25. **Kaneto H.** 2005. The JNK pathway as a therapeutic target for diabetes. Expert Opin. Ther. Targets **9**:581–592.
26. **Kayser JP, Vallet JL, Cerny RL.** 2004. Defining parameters for homology-tolerant database searching. J. Biomol. Tech. **15**:285–295.
27. **Kerscher O, Felberbaum R, Hochstrasser M.** 2006. Modification of proteins by ubiquitin and ubiquitin-like proteins. Annu. Rev. Cell Dev. Biol. **22**:159–180.
28. **Keshet Y, Seger R.** 2010. The MAP kinase signaling cascades: a system of hundreds of components regulates a diverse array of physiological functions. Methods Mol. Biol. **661**:3–38.
29. **Kluwe J, et al.** 2010. Modulation of hepatic fibrosis by c-Jun-N-terminal kinase inhibition. Gastroenterology **138**:347–359.
30. **Kook SH, et al.** 2008. Inhibition of c-Jun N-terminal kinase sensitizes tumor cells to flavonoid-induced apoptosis through down-regulation of JunD. Toxicol. Appl. Pharmacol. **227**:468–476.
31. **Kubo T, et al.** 2011. Oncolytic vesicular stomatitis virus administered by isolated limb perfusion suppresses osteosarcoma growth. J. Orthop. Res. **29**:795–800.
32. **Kyriakis JM, Avruch J.** 2001. Mammalian mitogen-activated protein kinase signal transduction pathways activated by stress and inflammation. Physiol. Rev. **81**:807–869.
33. **Lambert PJ, et al.** 2007. Targeting the PI3K and MAPK pathways to treat Kaposi's-sarcoma-associated herpes virus infection and pathogenesis. Expert Opin. Ther. Targets **11**:589–599.
34. **Liu JR, et al.** 2010. The c-Jun N-terminal kinase (JNK) inhibitor XG-102 enhances the neuroprotection of hyperbaric oxygen after cerebral ischaemia in adult rats. Neuropathol. Appl. Neurobiol. **36**:211–224.
35. **Liu M, et al.** 2007. Discovery of a new class of 4-anilinopyrimidines as potent c-Jun N-terminal kinase inhibitors: synthesis and SAR studies. Bioorg. Med. Chem. Lett. **17**:668–672.
36. **Llovet JM, Bruix J.** 2008. Molecular targeted therapies in hepatocellular carcinoma. Hepatology **48**:1312–1327.
37. **Lu YY, Chen TS, Wang XP, Qu JL, Chen M.** 2010. The JNK inhibitor SP600125 enhances dihydroartemisinin-induced apoptosis by accelerat-

ing Bax translocation into mitochondria in human lung adenocarcinoma cells. FEBS Lett. **584**:4019–4026.
38. **Marozin S, et al.** 2008. Inhibition of the IFN-beta response in hepatocellular carcinoma by alternative spliced isoform of IFN regulatory factor-3. Mol. Ther. **16**:1789–1797.
39. **Mizutani T, Fukushi S, Saijo M, Kurane I, Morikawa S.** 2005. JNK and PI3k/Akt signaling pathways are required for establishing persistent SARS-CoV infection in Vero E6 cells. Biochim. Biophys. Acta **1741**:4–10.
40. **Montagut C, Settleman J.** 2009. Targeting the RAF-MEK-ERK pathway in cancer therapy. Cancer Lett. **283**:125–134.
41. **Mucha SR, et al.** 2009. JNK inhibition sensitises hepatocellular carcinoma cells but not normal hepatocytes to the TNF-related apoptosis-inducing ligand. Gut **58**:688–698.
42. **Nagata H, et al.** 2009. Inhibition of c-Jun NH2-terminal kinase switches Smad3 signaling from oncogenesis to tumor-suppression in rat hepatocellular carcinoma. Hepatology **49**:1944–1953.
43. **Noser JA, et al.** 2007. The RAS/Raf1/MEK/ERK signaling pathway facilitates VSV-mediated oncolysis: implication for the defective interferon response in cancer cells. Mol. Ther. **15**:1531–1536.
44. **Nussler A, et al.** 2009. Regenerative medicine today: the holy grail of hepatocyte culturing and therapeutic use. Springer, Brighton, United Kingdom.
45. **Oliere S, et al.** 2008. Vesicular stomatitis virus oncolysis of T lymphocytes requires cell cycle entry and translation initiation. J. Virol. **82**:5735–5749.
46. **Pleschka S.** 2008. RNA viruses and the mitogenic Raf/MEK/ERK signal transduction cascade. Biol. Chem. **389**:1273–1282.
47. **Roberts PJ, Der CJ.** 2007. Targeting the Raf-MEK-ERK mitogen-activated protein kinase cascade for the treatment of cancer. Oncogene **26**:3291–3310.
48. **Salsman J, Top D, Barry C, Duncan R.** 2008. A virus-encoded cell-cell fusion machine dependent on surrogate adhesins. PLoS Pathog. **4**:e1000016.
49. **Schmidt CM, McKillop IH, Cahill PA, Sitzmann JV.** 1997. Increased MAPK expression and activity in primary human hepatocellular carcinoma. Biochem. Biophys. Res. Commun. **236**:54–58.
50. **Schwartz DC, Hochstrasser M.** 2003. A superfamily of protein tags: ubiquitin, SUMO and related modifiers. Trends Biochem. Sci. **28**:321–328.
51. **Shin EC, et al.** 2002. Human hepatocellular carcinoma cells resist to TRAIL-induced apoptosis, and the resistance is abolished by cisplatin. Exp. Mol. Med. **34**:114–122.
52. **Shinozaki K, Ebert O, Woo SL.** 2005. Eradication of advanced hepatocellular carcinoma in rats via repeated hepatic arterial infusions of recombinant VSV. Hepatology **41**:196–203.
53. **Shinozaki K, et al.** 2004. Oncolysis of multifocal hepatocellular carcinoma in the rat liver by hepatic artery infusion of vesicular stomatitis virus. Mol. Ther. **9**:368–376.
54. **Si X, et al.** 2005. Stress-activated protein kinases are involved in coxsackievirus B3 viral progeny release. J. Virol. **79**:13875–13881.
55. **Wang Y, Pernet O, Lee B.** 2012. Regulation of the nucleocytoplasmic trafficking of viral and cellular proteins by ubiquitin and small ubiquitin-related modifiers. Biol. Cell **104**:121–138.
56. **Wei L, Zhu Z, Wang J, Liu J.** 2009. JNK and p38 mitogen-activated protein kinase pathways contribute to porcine circovirus type 2 infection. J. Virol. **83**:6039–6047.
57. **Weston CR, Davis RJ.** 2007. The JNK signal transduction pathway. Curr. Opin. Cell Biol. **19**:142–149.
58. **Whitt MA, Zagouras P, Crise B, Rose JK.** 1990. A fusion-defective mutant of the vesicular stomatitis virus glycoprotein. J. Virol. **64**:4907–4913.
59. **Wimmer P, Schreiner S, Dobner T.** 2012. Human pathogens and the host cell SUMOylation system. J. Virol. **86**:642–654.
60. **Yu JH, Lin BY, Deng W, Broker TR, Chow LT.** 2007. Mitogen-activated protein kinases activate the nuclear localization sequence of human papillomavirus type 11 E1 DNA helicase to promote efficient nuclear import. J. Virol. **81**:5066–5078.
61. **Zapata HJ, Nakatsugawa M, Moffat JF.** 2007. Varicella-zoster virus infection of human fibroblast cells activates the c-Jun N-terminal kinase pathway. J. Virol. **81**:977–990.

AAC
Journals.ASM.org

ENT1, a Ribavirin Transporter, Plays a Pivotal Role in Antiviral Efficacy of Ribavirin in a Hepatitis C Virus Replication Cell System

Minami Iikura,[a] Tomomi Furihata,[a] Misa Mizuguchi,[a] Miki Nagai,[a] Masanori Ikeda,[b] Nobuyuki Kato,[b] Akihito Tsubota,[c] and Kan Chiba[a]

Laboratory of Pharmacology and Toxicology, Graduate School of Pharmaceutical Sciences, Chiba University, Chiba, Japan[a]; Department of Tumor Virology, Okayama University Graduate School of Medicine, Dentistry, and Pharmaceutical Science, Okayama, Japan[b]; and Institute of Clinical Medicine and Research, Jikei University School of Medicine, Chiba, Japan[c]

We previously showed that equilibrative nucleoside transporter 1 (ENT1) is a primary ribavirin transporter in human hepatocytes. However, because the role of this transporter in the antiviral mechanism of the drug remains unclear, the present study aimed to elucidate the role of ENT1 in ribavirin antiviral action. OR6 cells, a hepatitis C virus (HCV) replication system, were used to evaluate both ribavirin uptake and efficacy. The ribavirin transporter in OR6 cells was identified by mRNA expression analyses and transport assays. Nitrobenzylmercaptopurine riboside (NBMPR) and micro-RNA targeted to ENT1 mRNA (miR-ENT1) were used to reduce the ribavirin uptake level in OR6 cells. Our results showed that ribavirin antiviral activity was associated with its accumulation in OR6 cells, which was also closely associated with the uptake of the drug. It was found that the primary ribavirin transporter in OR6 cells was ENT1 and that inhibition of ENT1-mediated ribavirin uptake by NBMPR significantly attenuated the antiviral activity of the drug as well as its accumulation in OR6 cells. The results also showed that even a small reduction in the ENT1-mediated ribavirin uptake, achieved in this case using miR-ENT1, caused a significant decrease in its antiviral activity, thus indicating that the ENT1-mediated ribavirin uptake level determined its antiviral activity level in OR6 cells. In conclusion, our results show that by facilitating its uptake and accumulation in OR6 cells, ENT1 plays a pivotal role in the antiviral effectiveness of ribavirin and therefore provides an important insight into the efficacy of the drug in anti-HCV therapy.

Chronic hepatitis C is a major cause of liver cirrhosis and hepatocellular carcinoma, and a combination of interferon-α (IFN-α) and ribavirin is a standard anti-hepatitis C virus (HCV) therapy. Since the addition of ribavirin to IFN-α significantly improves the rate of sustained virologic response (SVR) (40 to 60% in genotype 1 patients) (5), the drug plays a key role in current anti-HCV therapy.

Ribavirin, a purine nucleoside analog, is phosphorylated intracellularly to form mono-, di-, and tri-phosphates, which then accumulate within cells at high concentrations (4, 13). While the primary anti-HCV mechanisms of the drug are still under debate, it is considered likely that the important actions take place within the cells themselves, and several mechanisms have been proposed to explain what occurs there. These include inhibition of inosine monophosphate dehydrogenase (reviewed in references 4 and 7 and references therein). Additionally, a recent study revealed that ribavirin potentiates IFN-α action by augmenting IFN-stimulated induction of gene expression (16).

Taking into consideration the above-mentioned mechanisms, it is reasonable to assume that the uptake of ribavirin into hepatocytes is a prerequisite for its antiviral activity. Since ribavirin is a hydrophilic molecule, import of the drug into cells requires host nucleoside transporters, which are divided into two families: equilibrative nucleoside transporters (such as ENT1 to ENT4) and concentrative nucleoside transporters (such as CNT1 to CNT3) (9). ENTs are facilitated transporters, while CNTs are sodium-dependent active transporters. These transporters differ in tissue distribution, substrate preference, and inhibitor sensitivity. For example, sensitivities to inhibition by nitrobenzylmercaptopurine riboside (NBMPR) are different between ENT1 and ENT2 (20).

Our recent investigations into the ribavirin uptake system in human hepatocytes determined that ENT1 is a primary ribavirin uptake transporter (6). In addition, Morello et al. (12) reported the association of an intronic single nucleotide polymorphism (SNP) of the *SLC29A1* (ENT1) gene with rapid virologic response (RVR; defined as an undetectable serum HCV RNA level at week 4) of treatment of genotype-1 Caucasian patients. More recently, Tsubota and colleagues revealed that another intronic SNP in the *SLC29A1* gene is associated with SVR, as well as RVR, in genotype-1 Japanese patients (18). Based on these findings, it can be hypothesized that ENT1 plays an essential role in ribavirin anti-HCV activity.

In the present study, along with a detailed characterization of ribavirin uptake and its relationship to antiviral activity, we tested the above-mentioned hypothesis through the use of OR6 cells, which have been established as an efficient replication system for the HCV RNA genome. The HCV replication level was evaluated by monitoring the level of *Renilla* luciferase activity (8), which enabled us to simultaneously evaluate both ribavirin uptake and its antiviral activity.

MATERIALS AND METHODS

Cell culture. OR6 cells were cloned from ORN/C-5B/KE cells (derived from Huh-7 cells) supporting genome-length HCV RNA (strain O of

Received 20 September 2011 **Returned for modification** 24 October 2011
Accepted 27 December 2011
Published ahead of print 9 January 2012
Address correspondence to Tomomi Furihata, tomomif@faculty.chiba-u.jp.
Supplemental material for this article may be found at http://aac.asm.org/.

doi:10.1128/AAC.05762-11

genotype 1b) containing the *Renilla* luciferase reporter gene, and the cells were cultured as described previously (8). Huh-7 cells were obtained from the Institute of Development, Aging and Cancer, Tohoku University (Sendai, Japan). The Huh-7 cells were cultured at 37°C with 5% CO_2–95% air in RPMI 1640 medium (Invitrogen, Carlsbad, CA) with 10% fetal bovine serum, 50 U/ml penicillin, and 50 μg/ml streptomycin.

Luciferase reporter assay. OR6 cells were plated 1 day prior to the assay on 24-well plates at 1.5×10^4 to 2.5×10^4 cells/well, followed by treatment with ribavirin (Wako, Osaka, Japan) in the absence of G418 and at the indicated concentrations for 24, 48, and 72 h. The cells were then subjected to the luciferase assay using a dual-luciferase reporter assay system (Promega, Madison, WI) according to the manufacturer's protocol. For data normalization, the protein contents were determined with a Pierce 660-nm protein assay reagent (Thermo Fisher Scientific, Rockford, IL) according to the manufacturer's protocol. The relative luciferase activity value of the untreated or vehicle treated cells (dimethyl sulfoxide [DMSO] for NBMPR and sterile water for others) was set to 100%. NBMPR (Sigma, St. Louis, MO), hypoxanthine (MP Biomedicals, Solon, OH), and formycin B (Berry & Associates, Ann Arbor, MI) were included in inhibition analyses at various concentrations.

Western blot analysis. OR6 cells treated with ribavirin at various concentrations in the absence of G418 for 24, 48, and 72 h were harvested and homogenized. The homogenates (60 μg/well) were resolved in a sodium dodecyl sulfate (SDS)–15% polyacrylamide gel and then transferred onto a nitrocellulose membrane. The membrane was blocked with 5% skim milk and then incubated with either antibodies against the HCV core protein (2,000-fold dilution; Institute of immunology, Tokyo, Japan) or antibodies against β-actin (500-fold dilution; Sigma). Immunocomplexes were detected with enhanced chemiluminescence (ECL) Western blotting detection reagents (GE Healthcare, Giles, United Kingdom).

Accumulation assay. OR6 cells were plated 1 day prior to the assay on 24-well plates, after which the cells were incubated with 0.5 μCi/ml [^{3}H]ribavirin (Moravek Biochemicals, Brea, CA) and nonradiolabeled ribavirin at various concentrations. NBMPR was included in inhibition analyses at concentrations of 0.1, 1, 3, 10, 31, and 100 μM. After treatment for 9.6, 24, 48, or 72 h, the cells were washed twice with ice-cold Na^+-free Krebs-Henseleit buffer (KHB) and lysed with 0.2% SDS. Radioactivity was measured using a liquid scintillation counter (LSC 5100; Aloka, Tokyo, Japan). The protein contents were determined as described above. To completely inhibit ENT-mediated ribavirin uptake, 30 μM dipyridamole (Wako) was used in the same experimental sets (20). The data were calculated by subtracting the accumulation values obtained with dipyridamole from those without dipyridamole at the same ribavirin concentrations. All assays were performed at 37°C.

Transport assays. Transport assays were performed using the previously described centrifugal filtration method (6). OR6 cells were collected and resuspended in ice-cold Na^+-containing KHB or Na^+-free KHB at 1.4×10^6 cells/ml. NBMPR, troglitazone (Wako), hypoxanthine, and formycin B were included in the inhibition analyses. Since the rate of ribavirin uptake by OR6 cells was linear for at least 60 s in the preliminary assays, the incubation time was set to 30 s. The radioactivity and protein contents of the cells used in the assay were measured as described above. The same experiments were also performed at 4°C, and the data were obtained by subtracting the uptake levels at 4°C from those at 37°C at the same ribavirin concentrations.

Total RNA preparation, cDNA synthesis, reverse transcription-PCR (RT-PCR), and quantitative real-time PCR (qPCR). Total RNA preparation, cDNA synthesis, RT-PCR, and qPCR were performed using previously described procedures (6). Among the nucleoside transporters, ENT1, ENT2, CNT2, and CNT3 mRNAs were examined by RT-PCR because they have been identified as ribavirin transporters (21). The primers for RT-PCR and qPCR are listed in Table S1 in the supplemental material. The UPL universal probes used were no. 9 (ENT1), no. 48 (ENT2), and no. 60 (glyceraldehyde 3-phosphate dehydrogenase [GAPDH]).

Knockdown of ENT1 mRNA expression in OR6 cells. The BLOCK-iT Pol II miR RNAi expression vector kit (Invitrogen) was used to suppress ENT1 mRNA expression in OR6 cells. The oligonucleotide containing micro-RNA targeted to ENT1 mRNA (miR-ENT1) was cloned into the pcDNA6.2-GW/EmGFP-miR vector. The control plasmid pcDNA6.2-GW/EmGFP-miR-neg, carrying an insert that is not known to target any identified vertebrate genes (miR-Neg), was used as a negative control. The sequences of inserts are shown in Table S1 in the supplemental material. The plasmids were transfected into OR6 cells using Lipofectamine LTX (Invitrogen). Two days after transfection, the culture medium was replaced with fresh medium containing 4 μg/ml blasticidin to obtain cells stably expressing miR-ENT1 (OR6/miR-ENT1) and cells stably expressing miR-Neg (OR6/miR-Ng).

Data analysis. Statistical analysis was performed using Student's *t* test. The four-parameter logistic model was used to calculate the 50% effective concentration (EC_{50}).

RESULTS

Concentration- and time-dependent anti-HCV activity and accumulation of ribavirin in OR6 cells. The inhibitory effects of ribavirin (1 to 3,162 μM) on HCV replication in OR6 cells were analyzed by monitoring the luciferase activity and HCV core protein expression levels. It was found that the HCV replication activity and core protein levels decreased in a ribavirin concentration-dependent manner (Fig. 1A and B), while the level of ribavirin accumulation increased in a saturable manner (Fig. 1C). Next, the time course of anti-HCV activity of ribavirin at concentrations of 10, 100, and 1,000 μM was examined. The results of our examination showed that, similar to the concentration-dependent profile, the HCV replication activity and core protein amounts decreased over time at each of the ribavirin concentrations tested (Fig. 1D and E) and that the levels of ribavirin accumulation increased linearly or saturably over time (Fig. 1F). These results suggest that ribavirin exerts concentration- and time-dependent antiviral activity that could be associated with the concentration- and time-dependent intracellular accumulation of the drug.

Identification of the ribavirin uptake transporter in OR6 cells. To identify the ribavirin uptake transporter in OR6 cells, we characterized the uptake profile of the drug and the nucleoside transporters mRNA expression in the cells. The ribavirin (1 to 3,162 μM) uptake level in Na^+-plus KHB was found to increase linearly up to 3 mM (Fig. 2A), and the uptake activities of the drug (nmol/mg protein/30 s) at 10, 100 (data not shown), and 1,000 μM were recorded as 0.03 ± 0.01, 0.33 ± 0.02 and 3.2 ± 0.3, respectively (Fig. 2B). The removal of Na^+ from the transport medium did not affect the uptake activities at any of the ribavirin concentrations tested, indicating that all the uptake activities of the drug were sodium independent. These activities were mostly abolished by the addition of 100 μM NBMPR, an inhibitor of ENT1 and ENT2. Consistently, the results of RT-PCR showed that ENT1 and ENT2 mRNAs were abundantly expressed in OR6 cells, while hardly any CNT2 and CNT3 mRNAs were expressed (Fig. 2C). During the above-described experiments, we found that a low concentration of NBMPR (100 nM) failed to inhibit ribavirin uptake by OR6 cells (M. Iikura, unpublished data). Considering that ENT1-mediated nucleoside uptake is generally sensitive to NBMPR inhibition at 100 nM (20), it was hypothesized that ENT2 should have contributed to ribavirin uptake in OR6 cells. However, our previous results indicated that ENT2 cannot transport ribavirin (6). Therefore, to clearly distinguish between ENT1- and

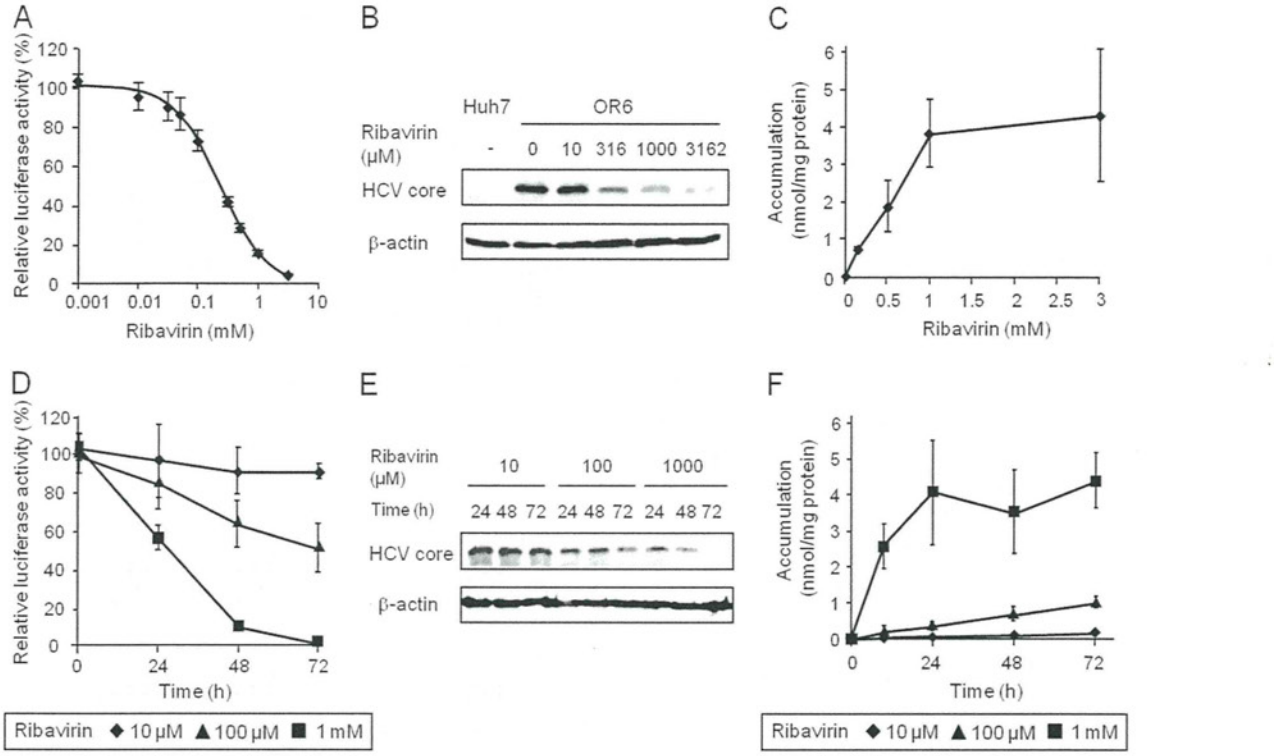

FIG 1 Concentration- and time-dependent profiles of anti-HCV activity and accumulation of ribavirin in OR6 cells. (A) OR6 cells were treated with ribavirin at concentrations of 0, 1, 10, 31, 50, 100, 316, 500, 1,000 and 3,162 μM for 48 h. The value of relative luciferase activity in the absence of ribavirin was set to 100%. (B) Expression levels of HCV core protein in OR6 cells treated with ribavirin for 48 h were examined by Western blot analysis. β-Actin was used as a loading control. Huh-7 cells were used as a negative control. (C) OR6 cells were treated with ribavirin at concentrations of 0.1, 0.5, 1, and 3 mM for 48 h, after which the radioactivity within the cells was determined. (D) OR6 cells were treated with ribavirin. The value of relative luciferase activity in the absence of ribavirin at each time point was set to 100%. (E) Expression levels of HCV core protein in OR6 cells treated with ribavirin were examined by Western blot analysis. (F) OR6 cells were treated with ribavirin, after which the radioactivity within the cells was determined. Values are means and standard deviations (SD) of the relative luciferase activity or the accumulation for three independent experiments. Each experiment was performed in duplicate. For Western blotting, the representative result for three independent assays was shown.

ENT2-mediated ribavirin uptake, inhibition analysis was performed using troglitazone (60 μM), hypoxanthine (5 mM), and formycin B (50 μM). Troglitazone has been reported to specifically inhibit ENT1 activity (10). Hypoxanthine and formycin B, at the indicated concentrations, were previously reported to preferentially inhibit ENT2 activity (3, 22), and we confirmed the inhibitory effects of these compounds on ENT2 activity by using HeLa cells (see Fig. S1 in the supplemental material). The results of the inhibition analysis showed that troglitazone completely inhibited the ribavirin uptake activity, while neither hypoxanthine nor formycin B inhibited uptake of the drug in OR6 cells (Fig. 2D). Taken together, the results indicated that, even though the affinity of ENT1 of OR6 cells for NBMPR was somehow reduced, ENT1 was exclusively responsible for the ribavirin uptake in OR6 cells.

Effect of inhibition of ribavirin uptake on its anti-HCV activity. After it was determined that ENT1 was responsible for ribavirin uptake in OR6 cells, the role of ENT1 in the anti-HCV activity of the drug (100 μM and 1 mM) was examined by chemical inhibition of ENT1-mediated ribavirin uptake in OR6 cells. Since troglitazone itself somewhat repressed HCV replication in OR6 cells (Iikura, unpublished), NBMPR was used as an ENT1 inhibitor. As shown in Fig. 3A, NBMPR decreased the level of ribavirin uptake in a dose-dependent manner and, accordingly, decreased the accumulation level of the drug in a dose-dependent manner (Fig. 3B). In association with these decreases, it was determined that the ribavirin antiviral effect was weakened by NBMPR in a concentration-dependent manner (Fig. 3C). We confirmed that ENT1 protein expression was not changed in the cells treated with the highest ribavirin and NBMPR concentrations for 48 h (see Fig. S2 in the supplemental material). To further clarify the importance of ENT1-mediated ribavirin uptake in its antiviral effects, the concentration and time dependencies of the antiviral effects of the drug were examined in cells treated with NBMPR or its vehicle (0.1% DMSO). The concentration of NBMPR was set to 7 μM, which is near the EC_{50} against ENT1 activity calculated from the results of Fig. 3A, indicating that the ENT1 activity level of NBMPR-treated cells was approximately half that of the vehicle-treated cells. As shown in Fig. 3D, the EC_{50} of ribavirin in the NBMPR-treated cells was 399 $\pm$ 22 μM, which was significantly higher than that of the vehicle-treated cells (203 $\pm$ 47 μM, P = 0.0005) (The results of the individual experiments are shown in Fig. S3 in the supplemental material.) In addition, the response to ribavirin in the NBMPR-treated cells was significantly delayed in comparison to that in the vehicle-treated cells (Fig. 3E). We also examined the constraining effects of ENT2 inhibitors on ribavirin antiviral activity but found that hypoxanthine (5 mM) and formycin B (50 μM) had no effect (see Fig. S4 in the supplemental material). Furthermore, NBMPR, hypoxanthine and formycin B

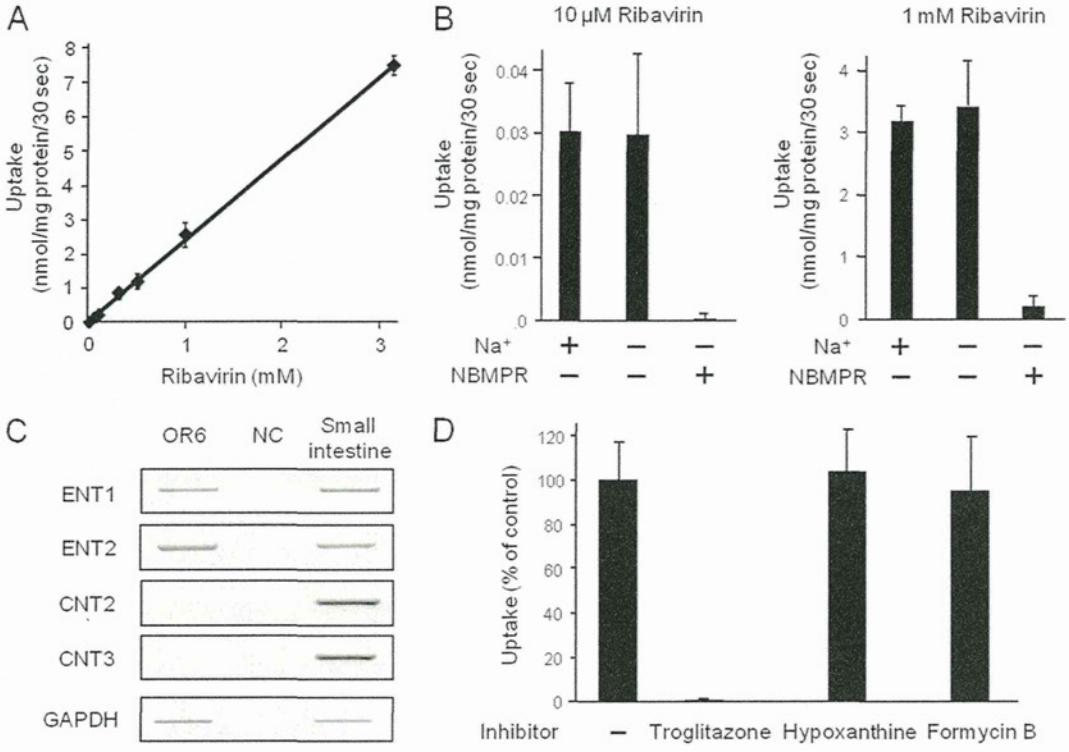

FIG 2 Identification of the ribavirin uptake transporter in OR6 cells. (A) The concentration dependence of ribavirin uptake (concentrations are given in the legend to Fig. 1A) by OR6 cells was analyzed in Na^+-containing KHB. (B) Ribavirin uptake by OR6 cells was analyzed in Na^+-containing KHB and Na^+-free KHB. In inhibition assays, the effect of 100 μM NBMPR on ribavirin uptake was analyzed in Na^+-free KHB. (C) ENT1, ENT2, CNT2, CNT3 and GAPDH mRNA expression was examined by RT-PCR. Small intestine cDNA was used as a PCR control. NC, nontemplate control. Representative results from one of three independent analyses are shown. (D) To clearly distinguish between ENT1- and ENT2-mediated ribavirin uptake, inhibition analysis of ribavirin (100 μM) uptake by OR6 cells was performed in Na^+-free KHB in the absence of inhibitor (−) or the presence of troglitazone (ENT1 inhibitor, 60 μM), hypoxanthine (ENT2 inhibitor, 5 mM), or formycin B (ENT2 inhibitor, 50 μM). The value of the transport activity of the control (no inhibitor) was set to 100%. In the above-described experiments, each value is the mean plus SD from three independent experiments, each performed in duplicate.

were found to have no effect on HCV replication activity in the above-described experiments (see Fig. S4 in the supplemental material), and NBMPR (7 μM) failed to affect telaprevir antiviral activity (see Fig. S5 in the supplemental material).

These results clearly show that inhibition of ENT1-mediated ribavirin uptake significantly attenuates ribavirin antiviral effectiveness by reducing the accumulation level of the drug in the cells.

Effect of ENT1 mRNA knockdown on ribavirin anti-HCV activity. The above-mentioned results prompted us to investigate whether a small change in ENT1 activity would similarly affect ribavirin antiviral effectiveness. miRNA targeted to ENT1 mRNA was used in this examination. We found that when stably expressed in OR6 cells (OR6/miR-ENT1), miR-ENT1 reduced the ENT1 mRNA expression level to 72.5 ± 3.4% of that of the control cells (OR6/miR-Ng) without affecting the ENT2 mRNA expression level (Fig. 4A). Accordingly, the ribavirin uptake level in OR6/miR-ENT1 cells was about 66.7 ± 14.0% of that in OR6/miR-Ng cells (Fig. 4B). To determine the degree to which this ENT1 mRNA knockdown affected ribavirin antiviral action, concentration dependencies of ribavirin action in OR6/miR-ENT1 and OR6/miR-Ng cells were characterized. We found that the EC_{50} of ribavirin in OR6/miR-ENT1 cells was 212 ± 11 μM, which was significantly higher than the EC_{50} in OR6/miR-Ng cells (143 ± 33 μM; $P = 0.013$) (The results of the individual experiments are shown in Fig. S3 in the supplemental material.) These results showed that even a small reduction in the ENT1 mRNA expression level could decrease the ribavirin uptake level, thus causing a reduction in the antiviral efficacy of the drug.

Toxicological analyses. Concurrent with the above-described experiments, the cytotoxic effects of ribavirin and other reagents on OR6 cells were examined independently and/or simultaneously (see the supplemental methods in the supplemental material). As shown in Table S2 and Fig. S6 of the supplemental materials, the lactate dehydrogenase (LDH) release assay results showed that no severe cytotoxicity in OR6 cells occurred in any treatments (less than 10%). Microscopic observation also showed that the cells were viable upon treatment with ribavirin (3,162 μM) together with NBMPR (100 μM) for 48 h (see Fig. S2 in the supplemental material). We further performed the MTS assay, which can detect different types of toxicity, to confirm the results of the LDH assay. The results showed that even though marginal toxicity was observed at the highest ribavirin and NBMPR concentrations tested (at most 25%), most treatments did not display severe cytotoxicity for OR6 cells (less than 10%; see Table S2 in the supplemental material).

DISCUSSION

In this paper, we provide results supporting our hypothesis that ENT1 plays an essential role in the anti-HCV activity of ribavirin

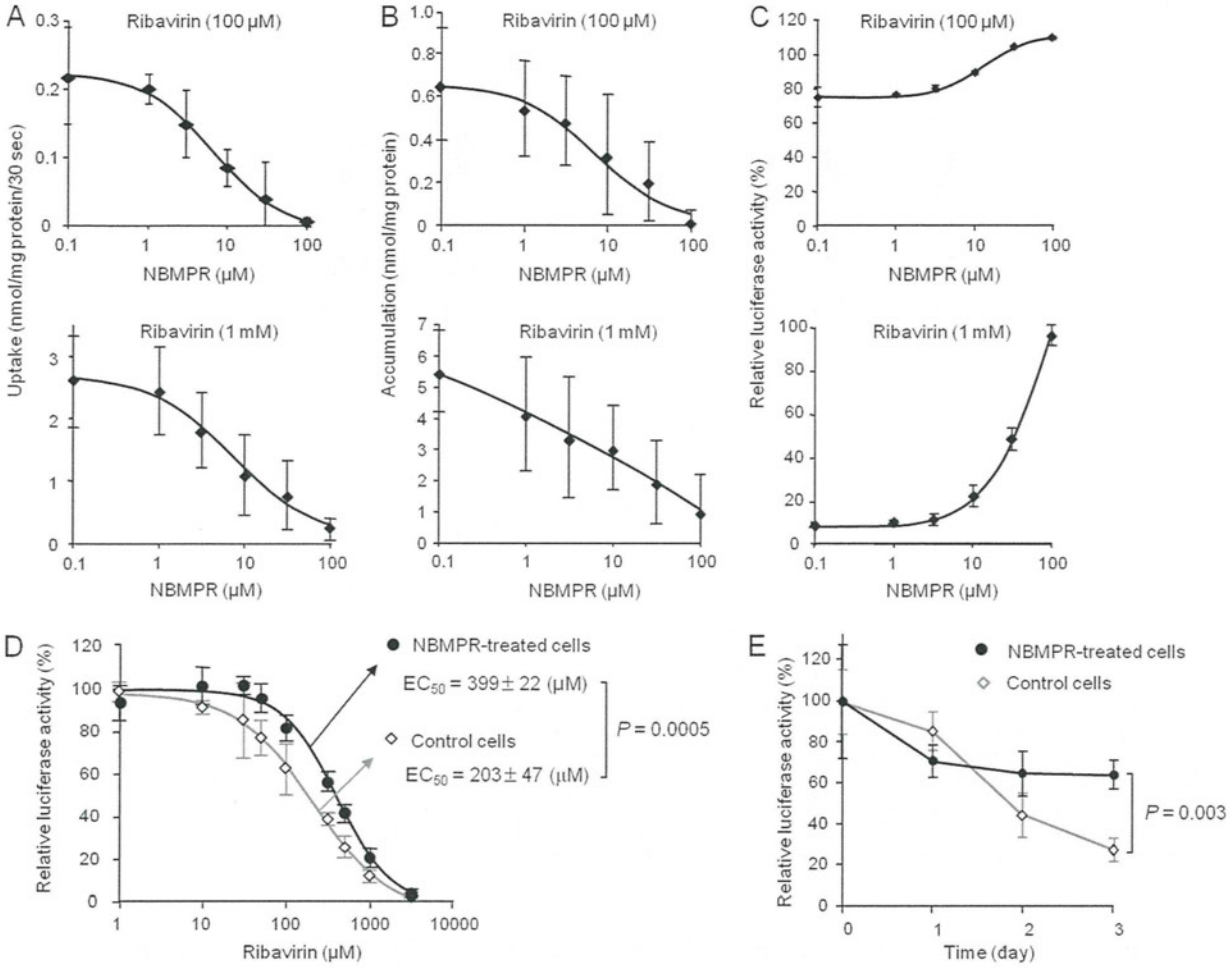

FIG 3 Inhibitory effect of NBMPR on ribavirin uptake, accumulation, and anti-HCV activity. The ribavirin concentration used in these experiments (A to C) was 100 μM or 1 mM, while the NBMPR concentrations used were 0.1, 1, 3, 10, 31, and 100 μM. (A) The effect of NBMPR on ribavirin uptake by OR6 cells was analyzed in Na^+-free KHB with NBMPR. Each value is the mean ± SD from five independent experiments, each performed in duplicate. (B) The effect of NBMPR on ribavirin accumulation in OR6 cells was analyzed by measuring the level of the drug within the cells, in the presence of NBMPR, for 48 h. Each value is the mean ± SD from three independent experiments, each performed in duplicate. (C) The effect of NBMPR on the anti-HCV activity of ribavirin in OR6 cells was analyzed by measuring the level of the luciferase activity, in the presence of NBMPR, for 48 h. The value of relative luciferase activity without ribavirin and NBMPR was set to 100%. Each value is the mean ± SD from three independent experiments, each performed in triplicate. (D) The concentration dependency of ribavirin antiviral action in the presence of NBMPR was examined. The ribavirin concentrations used are shown in the legend to Fig. 1A. The NBMPR concentration was set to 7 μM, which is near the EC_{50} of NBMPR calculated from the results in panel A. The value of relative luciferase activity in the absence of ribavirin was set to 100%. (E) The time dependency of ribavirin antiviral action in the presence of NBMPR was then examined. The ribavirin concentration was set to 150 μM, while the NBMPR concentration was still 7 μM. The value of relative luciferase activity in the absence of ribavirin at each time point was set to 100%.

through detailed characterization of the antiviral activity of the drug and its association with ENT1-mediated uptake in OR6 cells.

Our results showed that the concentration and time dependency of ribavirin antiviral activity was closely associated with its accumulation in OR6 cells. This association is supported by several reports. For example, it has been reported that larger ribavirin accumulations were associated with significant decreases in the intracellular GTP pool (13) or with higher antiviral potency against the Hantaan virus (14). Therefore, it is considered likely that continuous ribavirin accumulation in hepatic cells at the higher levels, which are achieved by the sustained and higher ribavirin extracellular concentrations, is critical to the antiviral efficacy of the drug.

Due to its hydrophilicity, ribavirin requires a "gate" to penetrate the plasma membrane of cells prior to its accumulation. Our results clearly show that ENT1 provides this gate, thus facilitating the drug's import into and accumulation in OR6 cells. Since we recently showed that ENT1 is also exclusively involved in ribavirin uptake in human hepatocytes, which has a ribavirin uptake profile similar to that of OR6 cells (6), it is considered likely that this ENT1 role can probably be extended to human hepatocytes as well. The mode of ENT1-mediated ribavirin uptake in OR6 cells, as well as human hepatocytes, was represented by a linear increase in the uptake level along with an increase in extracellular ribavirin concentration (6; also this study). This uptake feature was the most probable reason why the higher extracellular ribavirin concentration resulted in a stronger antiviral effect in OR6 cells but might also explain why clinical findings show that a higher exposure to ribavirin leads to the better virologic response in HCV genotype-1 patients (11, 17). Therefore, our results, together with

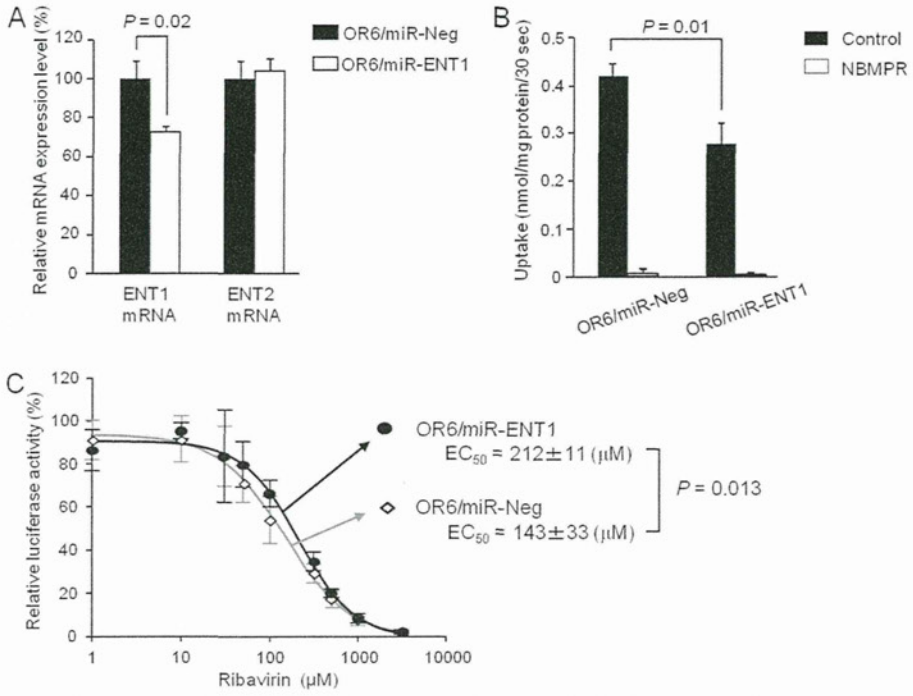

FIG 4 Effect of ENT1 mRNA knockdown on anti-HCV activity of ribavirin. (A) The expression levels of ENT1 and ENT2 mRNA were determined by real-time PCR. Abundance is shown relative to the level of ENT1 or ENT2 mRNA in OR6/miR-Ng cells. Each value is the mean plus SD from three independent experiments, each performed in duplicate. (B) Ribavirin (100 μM) uptake by OR6/miR-ENT1 and OR6/miR-Ng cells was analyzed in Na^+-free KHB in the absence (control) or presence of 100 μM NBMPR. Each value is the mean plus SD of transport activity from three independent experiments, each performed in duplicate. (C) The concentration dependency of ribavirin in OR6/miR-Ng and OR6/miR-ENT1 cells was then examined. The ribavirin concentrations used are shown in the legend to Fig. 1A. The relative luciferase activity value in the absence of ribavirin in each cell line was set to 100%. Each value is the mean ± SD of relative luciferase activity from four independent experiments, each performed in triplicate.

the other findings, indicate that ENT1 plays an indispensable role in ribavirin antiviral activity.

The importance of ENT1 in ribavirin antiviral activity was further underscored by the results of both the ENT1 knockdown and uptake inhibition experiments using NBMPR. It is noteworthy that even a small reduction of ENT1 activity significantly weakened ribavirin's antiviral potency. These results indicate that increasing or decreasing ENT1 activity level in the cells results in stronger or weaker ribavirin efficacy by increasing or reducing the uptake of the drug, even if extracellular ribavirin concentrations and exposure durations are constant. Therefore, it can be concluded that the ENT1-mediated ribavirin uptake level determines the level of ribavirin antiviral activity in OR6 cells and, presumably, in human hepatocytes.

The above-mentioned findings and suppositions prompt us to propose the following two possibilities (see Fig. S7 in the supplemental material). One is that patients with higher ENT1 activity levels in hepatocytes could more likely attain RVR (defined as a faster and stronger ribavirin antiviral effect in the early stage of the treatment) than those with lower ENT1 activity levels, when other factors affecting the treatment outcome are similar. The mechanisms underlying the interindividual difference in the hepatic ENT1 activity level remain unclear, but SNPs are promising candidates for the causal factors that result in the difference. Since two intronic SNPs have been revealed to be associated with RVR (and SVR) (12, 18), investigations should be conducted to determine whether these SNPs have a positive effect on the hepatic ENT1 expression level.

The other possibility is that the hepatic uptake of ribavirin by ENT1 could be hindered by coadministered chemicals, thus resulting in attenuation of the treatment response in some patients, as shown in Fig. 3. Although there have been no clinical reports supporting this possibility, preceding studies have been performed to determine whether hepatic uptake inhibition of pravastatin and metformin, which are hepatocyte-targeting drugs, reduces their effectiveness (1). These drugs are known substrates for hepatic organic ion transporters, and it has been shown that aberrations in these transporters significantly impair their *in vivo* functions (2, 15). Since, due to attendant complications or other chronic diseases, several drugs are often coprescribed along with ribavirin during treatment regimens, it may be worth considering whether interactions between ribavirin and other drugs at the point of ENT1-mediated uptake can affect the treatment response.

Exploration of these possibilities must await further studies aimed at clarification of the factors affecting the hepatic ENT1 activity level, including the above-described SNP studies and ribavirin-drug interaction studies. The results obtained from such studies could contribute not only to a better understanding of the mode of action of ENT1 on ribavirin antiviral activity but also to identification of the associated markers for RVR or null responses in clinical settings.

It should be noted that, unexpectedly, ENT1 activity was found to be insensitive to inhibition by NBMPR in the nanomolar range in OR6 cells. This was not due to nucleotide alterations in ENT1 cDNA of OR6 cells (Iikura, unpublished). Since OR6 cells were

derived from Huh-7 cells, we examined the sensitivity of ENT1 to inhibition of NBMPR using Huh-7 cells and obtained results similar to those obtained with OR6 cells (Iikura, unpublished). Therefore, the lower sensitivity of ENT1 to NBMPR in OR6 cells was thought to have originated from the Huh-7 cells. Although the reason for the altered sensitivity of ENT1 to NBMPR remains unknown at this time, it is believed that the cell-specific posttranslational modification might be involved. It has been reported that defective glycosylation of ENT1 leads to decreased affinity for NBMPR (19). Therefore, it can be speculated that the type or structure of glycochain and/or other modifications could be responsible for decreased affinity of ENT1 of OR6/Huh-7 cells for NBMPR. Further studies aimed at ascertaining the reason might provide novel insights into the biology of ENT1.

Finally, we briefly discuss the static cytotoxic effects of ribavirin and NBMPR on OR6 cells. According to the results of toxicological analyses, these reagents (at most concentrations tested) did not cause severe toxicity in OR6 cells (less than 10%), and only marginal toxicity was found in treatment of the reagents at the highest concentrations tested in an MTS assay. In contrast, blasticidin S treatment (20 ng/ml) significantly damaged the cells (>50% in the MTS assay [Iikura, unpublished]). Therefore, it is assumed that OR6 cells possess inherent resistance to ribavirin and NBMPR, and this factor might be related to the relatively high EC_{50} of ribavirin. Although we do not know the reason for the behavior of the cells, it is unlikely that the limited toxicity would give rise to a question regarding the present results. In actuality, 100 μM NBMPR treatment, which caused marginal toxicity, did not affect HCV replication activity (see Fig. S4 in the supplemental material).

In conclusion, we have clearly demonstrated that ENT1 plays an indispensable role in ribavirin antiviral activity by facilitating the uptake and accumulation of the drug in OR6 cells, thereby indicating that ENT1 provides a gate that is essential to the success of ribavirin's mission. Our study limitations include an *in vitro* HCV model system using hepatoma cells and no *in vivo* evidence of association between hepatic ENT1 activity and ribavirin efficacy. Nevertheless, our results, together with the literature, strongly suggest that ENT1 also plays the determinant role in the antiviral efficacy of ribavirin in the human liver during the course of anti-HCV therapy. Accordingly, it is believed that our results, as well as the ideas described in this paper, will encourage further studies aimed at the clarification of the clinical importance of ENT1 in anti-HCV therapy.

ACKNOWLEDGMENTS

This work was supported by a grant (20790128) from the Ministry of Education, Sciences, Sports and Culture of Japan and partially supported by a Special Funds for Education and Research (Development of SPECT Probes for Pharmaceutical Innovation) from the Ministry of Education, Culture, Sports, Science and Technology, Japan, and a research grant from the Nakatomi Foundation (Tokyo, Japan).

REFERENCES

1. **Bachmakov I, Glaeser H, Fromm MF, König J.** 2008. Interaction of oral antidiabetic drugs with hepatic uptake transporters: Focus on organic anion transporting polypeptides and organic cation transporter 1. Diabetes 57:1463–1469.
2. **Becker ML, et al.** 2009. Genetic variation in the organic cation transporter 1 is associated with metformin response in patients with diabetes mellitus. Pharmacogenomics J. 9:242–247.
3. **Burke T, Lee S, Ferguson PJ, Hammond JR.** 1998. Interaction of 2′,2′-difluorodeoxycytidine (gemcitabine) and formycin B with the Na^+-dependent and -independent nucleoside transporters of Ehrlich ascites tumor cells. J. Pharmacol. Exp. Ther. 286:1333–1340.
4. **Dixit NM, Perelson AS.** 2006. The metabolism, pharmacokinetics and mechanisms of antiviral activity of ribavirin against hepatitis C virus. Cell. Mol. Life Sci. 63:832–842.
5. **Fried MW, et al.** 2002. Peginterferon alfa-2a plus ribavirin for chronic hepatitis C virus infection. N. Engl. J. Med. 347:975–982.
6. **Fukuchi Y, Furihata T, Hashizume M, Iikura M, Chiba K.** 2010. Characterization of ribavirin uptake systems in human hepatocytes. J. Hepatol. 52:486–492.
7. **Hofmann WP, Herrmann E, Sarrazin C, Zeuzem S.** 2008. Ribavirin mode of action in chronic hepatitis C: from clinical use back to molecular mechanisms. Liver Int. 28:1332–1343.
8. **Ikeda M, et al.** 2005. Efficient replication of a full-length hepatitis C virus genome, strain O, in cell culture, and development of a luciferase reporter system. Biochem. Biophys. Res. Commun. 329:1350–1359.
9. **Kong W, Engel K, Wang J.** 2004. Mammalian nucleoside transporters. Curr. Drug Metab. 5:63–84.
10. **Leung GP, Man RY, Tse CM.** 2005. Effect of thiazolidinediones on equilibrative nucleoside transporter-1 in human aortic smooth muscle cells. Biochem. Pharmacol. 70:355–362.
11. **Lindahl K, Stahle L, Bruchfeld A, Schvarcz R.** 2005. High-dose ribavirin in combination with standard dose peginterferon for treatment of patients with chronic hepatitis C. Hepatology 41:275–279.
12. **Morello J, et al.** 2010. Influence of a single nucleotide polymorphism at the main ribavirin transporter gene on the rapid virological response to pegylated interferon-ribavirin therapy in patients with chronic hepatitis C virus infection. J. Infect. Dis. 202:1185–1191.
13. **Smee DF, Matthews TR.** 1986. Metabolism of ribavirin in respiratory syncytial virus-infected and uninfected cells. Antimicrob. Agents Chemother. 30:117–121.
14. **Sun Y, Chung DH, Chu YK, Jonsson CB, Parker WB.** 2007. Activity of ribavirin against Hantaan virus correlates with production of ribavirin-5′-triphosphate, not with inhibition of IMP dehydrogenase. Antimicrob. Agents Chemother. 51:84–88.
15. **Tachibana-Iimori R, et al.** 2004. Effect of genetic polymorphism of OATP-C (SLCO1B1) on lipid-lowering response to HMG-CoA reductase inhibitors. Drug Metab. Pharmacokinet. 19:375–380.
16. **Thomas E, et al.** 2011. Ribavirin potentiates interferon action by augmenting interferon-stimulated gene induction in hepatitis C virus cell culture models. Hepatology 53:32–41.
17. **Tsubota A, Hirose Y, Izumi N, Kumada H.** 2003. Pharmacokinetics of ribavirin in combined interferon-alpha 2b and ribavirin therapy for chronic hepatitis C virus infection. Br. J. Clin. Pharmacol. 55:360–367.
18. **Tsubota A, et al.** 2011. Contribution of ribavirin transporter gene polymorphism to treatment response in peginterferon plus ribavirin therapy for HCV genotype 1b patients. Liver Int. [Epub ahead of print.10.1111/j.1478–3231.2011.02727.x.
19. **Vickers MF, et al.** 1999. Functional production and reconstitution of the human equilibrative nucleoside transporter (hENT1) in Saccharomyces cerevisiae. Interaction of inhibitors of nucleoside transport with recombinant hENT1 and a glycosylation-defective derivative (hENT1/N48Q). Biochem. J. 339:21–32.
20. **Ward JL, Sherali A, Mo ZP, Tse CM.** 2000. Kinetic and pharmacological properties of cloned human equilibrative nucleoside transporters, ENT1 and ENT2, stably expressed in nucleoside transporter-deficient PK15 cells. J. Biol. Chem. 275:8375–8381.
21. **Yamamoto T, et al.** 2007. Ribavirin uptake by cultured human choriocarcinoma (BeWo) cells and Xenopus laevis oocytes expressing recombinant plasma membrane human nucleoside transporters. Eur. J. Pharmacol. 557:1–8.
22. **Yao SY, et al.** 2002. Functional and molecular characterization of nucleobase transport by recombinant human and rat equilibrative nucleoside transporters 1 and 2. J. Biol. Chem. 277:24938–24948.

Mar. Drugs **2012**, *10*, 744-761; doi:10.3390/md10040744

OPEN ACCESS

Marine Drugs

ISSN 1660-3397

www.mdpi.com/journal/marinedrugs

Article

Inhibition of Hepatitis C Virus Replication and Viral Helicase by Ethyl Acetate Extract of the Marine Feather Star *Alloeocomatella polycladia*

Atsuya Yamashita [1], Kazi Abdus Salam [2,†], Atsushi Furuta [3,4,†], Yasuyoshi Matsuda [3,4], Osamu Fujita [3,4], Hidenori Tani [2], Yoshihisa Fujita [5,6], Yuusuke Fujimoto [1], Masanori Ikeda [7], Nobuyuki Kato [7], Naoya Sakamoto [8], Shinya Maekawa [9], Nobuyuki Enomoto [9], Masamichi Nakakoshi [10], Masayoshi Tsubuki [10], Yuji Sekiguchi [3], Satoshi Tsuneda [4], Nobuyoshi Akimitsu [2], Naohiro Noda [3], Junichi Tanaka [11,*] and Kohji Moriishi [1,*]

[1] Department of Microbiology, Division of Medicine, Graduate School of Medicine and Engineering, University of Yamanashi, 1110 Shimokato, Chuo-shi, Yamanashi 409-3898, Japan; E-Mails: atsuyay@yamanashi.ac.jp (A.Y.); yfujimoto@yamanashi.ac.jp (Y.F.)

[2] Radioisotope Center, The University of Tokyo, 2-11-16 Yayoi, Bunkyo-ku, Tokyo 113-0032, Japan; E-Mails: salam_bio26@yahoo.com (K.A.S); tani@ric.u-tokyo.ac.jp (H.T.); akimitsu@ric.u-tokyo.ac.jp (N.A.)

[3] Biomedical Research Institute, National Institute of Advanced Industrial Science and Technology (AIST), 1-1-1 Higashi, Tsukuba, Ibaraki 305-8566, Japan; E-Mails: atsushi.furuta@aist.go.jp (A.F.); yellow-3359@hotmail.co.jp (Y.M.); 036.fujita@gmail.com (O.F.); y.sekiguchi@aist.go.jp (Y.S.); noda-naohiro@aist.go.jp (N.N.)

[4] Department of Life Science and Medical Bio-Science, Waseda University, 2-2 Wakamatsu-cho, Shinjuku-ku, Tokyo 162-8480, Japan; E-Mail: stsuneda@waseda.jp

[5] University Education Center, University of the Ryukyus, Okinawa, 1 Senbaru, Nishihara, Okinawa 903-0213, Japan; E-Mail: galatheids@yahoo.co.jp

[6] Marine Learning Center, 2-95-101 Miyagi, Chatan, Okinawa 901-0113, Japan

[7] Department of Tumor Virology, Okayama University Graduate School of Medicine, Dentistry, and Pharmaceutical Sciences, Okayama, 2-5-1 Shikata-cho, Okayama 700-8558, Japan; E-Mails: maikeda@md.okayama-u.ac.jp (M.I.); nkato@md.okayama-u.ac.jp (N.K.)

[8] Department of Gastroenterology and Hepatology, Tokyo Medical and Dental University, 1-5-45 Yushima, Bunkyo-ku, Tokyo, Japan; E-Mail: nsakamoto.gast@tmd.ac.jp

[9] First Department of Internal Medicine, Faculty of Medicine, University of Yamanashi, Yamanashi, 1110 Shimokato, Chuo-shi, Yamanashi 409-3898, Japan; E-Mails: maekawa@yamanashi.ac.jp (S.M); enomoto@yamanashi.ac.jp (N.E)

[10] Institute of Medical Chemistry, Hoshi University, Ebara 2-4-41, Shinagawa-ku, Tokyo 142-8501, Japan; E-Mails: mnakako@hoshi.ac.jp (M.N.); tsubuki@hoshi.ac.jp (M.T.)

[11] Department of Chemistry, Biology and Marine Science, University of the Ryukyus, Nishihara, Okinawa 903-0213, Japan

† These authors contributed equally to this work.

* Authors to whom correspondence should be addressed; E-Mails: jtanaka@sci.u-ryukyu.ac.jp (J.T.); kmoriishi@yamanashi.ac.jp (K.M.); Tel: +81-98-895-8560 (J.T.); +81-55-273-9537 (K.M.); Fax: +81-98-895-8565 (J.T.); Fax: +81-55-273-6728 (K.M.).

Received: 9 February 2012; in revised form: 17 March 2012 / Accepted: 19 March 2012 / Published: 28 March 2012

Abstract: Hepatitis C virus (HCV) is a causative agent of acute and chronic hepatitis, leading to the development of hepatic cirrhosis and hepatocellular carcinoma. We prepared extracts from 61 marine organisms and screened them by an *in vitro* fluorescence assay targeting the viral helicase (NS3), which plays an important role in HCV replication, to identify effective candidates for anti-HCV agents. An ethyl acetate-soluble fraction of the feather star *Alloeocomatella polycladia* exhibited the strongest inhibition of NS3 helicase activity, with an IC_{50} of 11.7 μg/mL. The extract of *A. polycladia* inhibited interaction between NS3 and RNA but not ATPase of NS3. Furthermore, the replication of the replicons derived from three HCV strains of genotype 1b in cultured cells was suppressed by the extract with an EC_{50} value of 23 to 44 μg/mL, which is similar to the IC_{50} value of the NS3 helicase assay. The extract did not induce interferon or inhibit cell growth. These results suggest that the unknown compound(s) included in *A. polycladia* can inhibit HCV replication by suppressing the helicase activity of HCV NS3. This study may present a new approach toward the development of a novel therapy for chronic hepatitis C.

Keywords: marine organism; *Alloeocomatella polycladia*; hepatitis C virus; NS3 helicase

---

1. Introduction

Hepatitis C virus (HCV) is an etiological agent of liver disease including steatosis, cirrhosis, and hepatocellular carcinoma, and has infected over 170 million individuals worldwide [1,2]. HCV belongs to the genus *Hepacivirus* of the *Flaviviridae* family. The genome of HCV is a single positive-strand RNA composed of 9.6 kb flanked by 5' and 3'-untranscribed regions (UTRs) and encodes a polyprotein consisting of approximately 3000 amino acids [3]. The polyprotein is translated from a viral genome by an internal ribosome entry site (IRES), which is localized in 5'-UTR [4]. The translated polyprotein is cleaved by host and viral proteases into 10 proteins. The structural proteins consisting of core, E1, and E2 and a viroporin p7, which has not yet been classified as either a structural or nonstructural protein, are located in the *N*-terminal quarter of the polyprotein. The nonstructural proteins including

NS2, NS3, NS4A, NS4B, NS5A, and NS5B occupy the remaining portion of the polyprotein and form a replication complex with several host factors.

HCV NS3 is well known to play a crucial role in viral replication because it possesses helicase and protease activities [5,6]. The *N*-terminal third of NS3 forms a complex with the NS4A protein and exhibits serine protease activity (NS3-4A protease) to cleave the viral polyprotein for the maturation of viral proteins [7]. The remaining portion of NS3 occupies the RNA helicase domain, characterized by the activities of ATPase and RNA binding, both of which contribute to the unwinding of duplex RNA [8,9]. The helicase activity is needed to separate duplex RNA during viral RNA replication [10]. A negative-strand RNA is synthesized based on a viral genome (positive strand) after the uncoating of a viral particle in the infected cells and then is itself used as a template to synthesize a positive-strand RNA packaged into the viral particle. Thus, helicase as well as protease activities of NS3 can be targeted for use in the development of antiviral agents against HCV.

The current therapy, which combines pegylated interferon with ribavirin, is effective in only about half of patients infected with the most common genotype worldwide, genotype 1 [11–13]. However, this therapy has side effects including influenza-like symptoms, cytopenias, and depression [11]. Furthermore, no effective vaccines for HCV have been developed yet. Biotechnological advances of the past decade have led to the development of novel therapies using anti-HCV agents that directly target HCV proteins or host factors required for HCV replication. This approach has been named either "specifically targeted antiviral therapy for hepatitis C" (STAT-C) or "directed-acting antiviral agents" (DAA) [14–16]. Several compounds of STAT-C or DAA have proceeded to clinical trials. Telaprevir and boceprevir, which are categorized as advanced NS3/4A protease inhibitors, were recently approved for the treatment of chronic hepatitis C patients infected with genotype 1 in the US, EU, Canada, and Japan [17,18]. However, the emergence of drug-resistant viruses is the major problem for therapies using antiviral compounds [19,20]. Accordingly, several kinds of drugs targeting various molecules or positions will be required for the complete eradication of the virus from hepatitis C patients.

The helicase activity of NS3 could be targeted by development of anti-HCV compound in addition to its protease activity. Belon *et al.* reported that 1-*N*,4-*N*-*bis*[4-(1*H*-benzimidazol-2-yl)phenyl] benzene-1,4-dicarboxamine, designated as $(BIP)_2B$, is a potent and selective inhibitor of HCV NS3 helicase [21]. $(BIP)_2B$ could not affect ATP hydrolysis without RNA or at a saturated concentration of RNA. QU663 inhibits the unwinding activity of NS3 helicase by binding to the RNA-binding groove irrespective of its own ATPase activity [22]. Compound QU663 may competitively bind the RNA-binding site of NS3 but not affect ATPase activity, resulting in the inhibition of unwinding activity.

Various drugs have been generated from natural products, especially those from terrestrial plants and microbes. The development of drugs from natural products has declined in the past two decades by the emergence of high-throughput screening of synthetic chemical libraries. However, recent technical advances in the determination of molecular structures and in the synthesis of chemical compounds have raised awareness about natural products as a resource for drug development [23–25]. Several groups recently reported natural products that inhibit HCV replication *in vitro*. For instance, silbinin, which is identified from the milk thistle [26,27], epigallocatechin 3-gallate, which is from green tea [28], and proanthocyanidins, which are from blueberry leaves [29], can inhibit HCV replication in cultured cells. Marine organisms including plants and animals were recently established as a representative natural resource library for drug development, since there are estimated to be more than 300,000

species of marine organisms. The products isolated from the marine organisms often possess potent biological activities corresponding to the organisms' own novel molecular structures. Thus, marine natural products are considered to include highly significant lead compounds for drug development [30,31]. For example, trabectedin (Yondelis), cytarabine (Ara-C), and eribulin (Halaven) are approved anticancer drugs developed from marine organisms [32]. However, marine organisms have not yet been screened for development into anti-HCV agents.

In this study, we screened extracts of marine organisms by using an *in vitro* fluorescence NS3 helicase assay and HCV replicon system to find candidates for safe and effective anti-HCV agents. The marine feather star *Alloeocomatella polycladia* may produce anti-HCV helicase agents that suppress HCV replication.

2. Results and Discussion

2.1. Primary Screening of Marine Organism Extracts on HCV NS3 Helicase Activity

We employed high-throughput screening using a photoinduced electron transfer (PET) assay to identify inhibitors of HCV NS3 helicase activity from extracts of marine organisms (Figure 1). The EtOAc- and MeOH-soluble extracts were prepared from marine organisms obtained from the sea around Okinawa Prefecture, Japan. We identified 16 extracts possessing an arbitrary level of inhibitory activity, which is defined as below 60% of the control in this study (Table 1). Five extracts exhibited high inhibition levels (<30%), and eleven extracts exhibited intermediate inhibition levels (30% to 60%). The EtOAc extract prepared from the feather star *Alloeocomatella polycladia* (Figure 2) exhibited the strongest inhibitory activity among them, and was designated SG1-23-1 in this study. Treatment with SG1-23-1 inhibited the helicase activity in a dose-dependent manner (Figure 3A). The value of IC_{50} is calculated as 11.7 ± 0.7 μg/mL. We confirmed the effect of SG1-23-1 on NS3 helicase unwinding activity by the RNA helicase assay using ^{32}P-labeled double-stranded RNA (dsRNA) as a substrate. Treatment with SG1-23-1 inhibited dsRNA dissociation at concentrations of 16 μg/mL and above (Figure 3B). These results suggest that treatment with SG1-23-1 inhibits the unwinding ability of HCV NS3 helicase.

Table 1. Inhibitory effects of marine organism extracts on hepatitis C virus (HCV) NS3 helicase activity.

Sample	Helicase Activity (% of control)	Specimen	Phylum	Extract	Collection Site
OK-99-2	78	*Agelas* sp.	Porifera	EtOAc	Shimoji Island
OK-99-3	73	*Plakortis* sp.	Porifera	EtOAc	Shimoji Island
OK-99-4	60	*Dysidea arenaria*	Porifera	EtOAc	Shimoji Island
OK-99-5	96	*Theonella cupola*	Porifera	EtOAc	Shimoji Island
OK-99-6	52	*Theonella conica*	Porifera	EtOAc	Shimoji Island
OK-99-7	85	*Epipolasis kushimotoensis*	Porifera	EtOAc	Shimoji Island
OK-99-9	51	*Hyrtios* sp.	Porifera	EtOAc	Shimoji Island

Table 1. *Cont.*

OK-99-10	75	*Theonella* sp.	Porifera	EtOAc	Shimoji Island
OK-99-12	53	*Isis hippuris*	Cnidaria	EtOAc	Shimoji Island
OK-99-13	68	*Acanthella* sp.	Porifera	EtOAc	Shimoji Island
OK-99-15	64	*Phyllospongia* sp.	Porifera	EtOAc	Shimoji Island
OK-99-17	59	*Petrosia* sp.	Porifera	EtOAc	Shimoji Island
OK-99-18	80	*Fasciospongia rimosa*	Porifera	EtOAc	Shimoji Island
OK-99-20	77	*Echinoclathria* sp.	Porifera	EtOAc	Shimoji Island
OK-99-21	68	*Strongylophora* sp.	Porifera	EtOAc	Shimoji Island
OK-99-23	74	*Dysidea herbacea*	Porifera	EtOAc	Shimoji Island
OK-99-26	55	*Dysidea* cf. *arenaria*	Porifera	EtOAc	Shimoji Island
OK-99-28	123	*Plakortis* sp.	Porifera	EtOAc	Shimoji Island
OK-99-31	118	*Spongia* sp.	Porifera	EtOAc	Okinawa Island
OK-99-34	119	*Theonella swinhoei*	Porifera	EtOAc	Okinawa Island
OK-99-35	108	*Petrosia* sp.	Porifera	EtOAc	Okinawa Island
OK-99-36	90	*Acanthella* sp.	Porifera	EtOAc	Okinawa Island
OK-99-37	102	*Luffariella* sp.	Porifera	EtOAc	Okinawa Island
OK-99-41	62	*Dysidea* cf. *arenaria*	Porifera	EtOAc	Okinawa Island
OK-99-43	85	*Xestospongia* sp.	Porifera	EtOAc	Okinawa Island
OK-99-44	61	*Dysidea arenaria*	Porifera	EtOAc	Okinawa Island
OK-99-47	108	*Dysidea* cf. *arenaria*	Porifera	EtOAc	Okinawa Island
OK-99-49	90	*Petrosia* sp.	Porifera	EtOAc	Chibishi
OK-99-51	69	*Isis hippuris*	Cnidaria	EtOAc	Chibishi
OK-99-52	78	*Petrosia* sp.	Porifera	EtOAc	Kuro Island
OK-99-55	65	*Acanthella* sp.	Porifera	EtOAc	Kuro Island
OK-99-57	84	*Theonella swinhoei*	Porifera	EtOAc	Kuro Island
OK-99-63	117	*Epipolasis kushimotoensis*	Porifera	EtOAc	Kuro Island
OK-99-64	98	*Xestospongia* sp.	Porifera	EtOAc	Kuro Island
SG1-1-2	77	*Comanthus gisleni*	Echinodermata	MeOH	Kume Island
SG1-2-2	112	*Stephanometra indica*	Echinodermata	MeOH	Kume Island
SG1-5-2	33	*Comantella* sp. cf. *maculata*	Echinodermata	MeOH	Kume Island
SG1-9-2	57	*Phanogenia gracilis*	Echinodermata	MeOH	Kume Island
SG1-12-2	39	*Comanthus parvicirrus*	Echinodermata	MeOH	Kume Island
SG1-14-2	117	*Comaster schlegelii*	Echinodermata	MeOH	Kume Island
SG1-15-2	26	Colobometridae sp.	Echinodermata	MeOH	Kume Island
SG1-16-2	66	*Cenometra bella*	Echinodermata	MeOH	Kume Island
SG1-19-2	78	*Comaster nobilis*	Echinodermata	MeOH	Kume Island
SG1-21-2	32	*Oxycomanthus* sp.	Echinodermata	MeOH	Kume Island
SG1-23-1	-3	*Alloeocomatella polycladia*	Echinodermata	EtOAc	Kume Island

Table 1. *Cont.*

SG1-24-1	24	*Comanthus* sp.	Echinodermata	EtOAc	Kume Island
SG1-26-2	51	*Oxycomanthus benetti*	Echinodermata	MeOH	Kume Island
SG1-28-2	38	*Lamprometra palmata*	Echinodermata	MeOH	Kume Island
SG1-30-1	25	*Colobometra perspinosa*	Echinodermata	EtOAc	Kume Island
SG1-31-1	26	*Comanthus* sp.	Echinodermata	EtOAc	Kume Island
SG1-33-1	32	*Basilometra boschmai*	Echinodermata	EtOAc	Kume Island
SG3-1	82	*Stereonephthya* sp.	Cnidaria	EtOAc	Tokashiki Island
SG3-4	73	*Dysidea* cf. *arenaria*	Porifera	EtOAc	Tokashiki Island
SG3-6	74	*Stylotella* sp.	Porifera	EtOAc	Tokashiki Island
SG3-10	139	*Epipolasis* sp.	Porifera	EtOAc	Tokashiki Island
SG3-11	97	*Nephthea* sp.	Cnidaria	EtOAc	Tokashiki Island
SG3-21	106	*Myrmekioderma* sp.	Porifera	EtOAc	Tokashiki Island
SG3-25	111	*Pseudoceratina purpurea*	Porifera	EtOAc	Tokashiki Island
SG3-26	95	*Leucetta* sp.	Porifera	EtOAc	Tokashiki Island
SG3-28	65	*Lyngbya* sp.	Cyanobacteria	EtOAc	Tokashiki Island
SG3-29	61	*Dysidea* sp.	Porifera	EtOAc	Tokashiki Island

Total number of marine organisms: 61; Marine organisms that strongly inhibit NS3 helicase activity (<30%) (boldface and underlined): 5; Extracts of organisms that exhibit intermediate inhibition of NS3 helicase activity (30%–60%) (underlined): 11; EtOAc: Ethyl acetate; MeOH: Methanol.

Figure 1. Schematic representation of the PET assay system for unwinding activity of HCV NS3 helicase. The fluorescent dye (BODIPY FL) is attached to the cytosine at the 5'-end of the fluorescent strand and quenched by the guanine base at the 3'-end of the complementary strand via photoinduced electron transfer. When the helicase unwinds the double-strand RNA substrate, the fluorescence of the dye emits bright light upon the release of the dye from the guanine base. The capture strand, which is complementary to the complementary strand, prevents the reannealing of the unwound duplex.

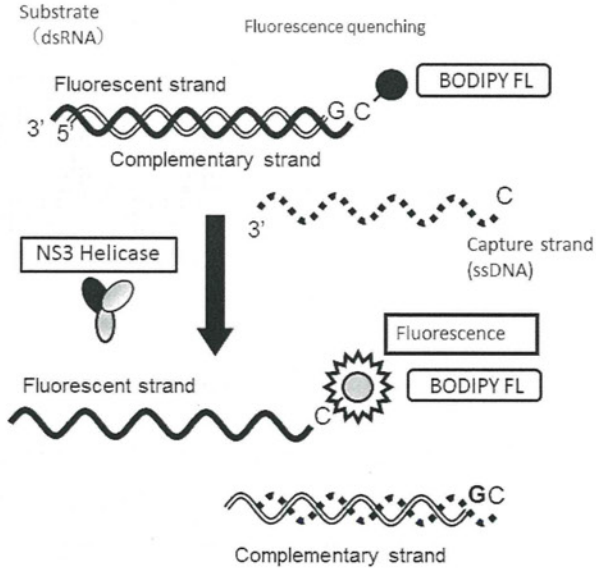

Figure 2. *Alloeocomatella polycladia* belongs to a class of feather star (Echinodermata, Crinoidea). The ethyl acetate fraction prepared from the marine organism was designated SG1-23-1 in this study.

Figure 3. Effect of SG1-23-1 on the unwinding activity of NS3 helicase. (**A**) NS3 helicase activity was measured by PET assay. The reactions were carried out in the absence or presence of SG1-23-1. Helicase activity in the absence of SG1-23-1 was defined as 100% helicase activity. Each value represents the mean of three independent reactions. Error bars indicate standard deviation. The data represent three independent experiments. (**B**) The unwinding activity of NS3 helicase was measured by RNA unwinding assay using radioisotope-labeled RNA. The heat-denatured single-strand RNA (26-mer) and the partial duplex RNA substrate were applied to lanes 1 and 2, respectively. The duplex RNA was reacted with NS3 (300 nM) in the presence of SG1-23-1 (lanes 4 to 9, 16 to 500 μg/mL). The resulting samples were subjected to native polyacrylamide gel electrophoresis.

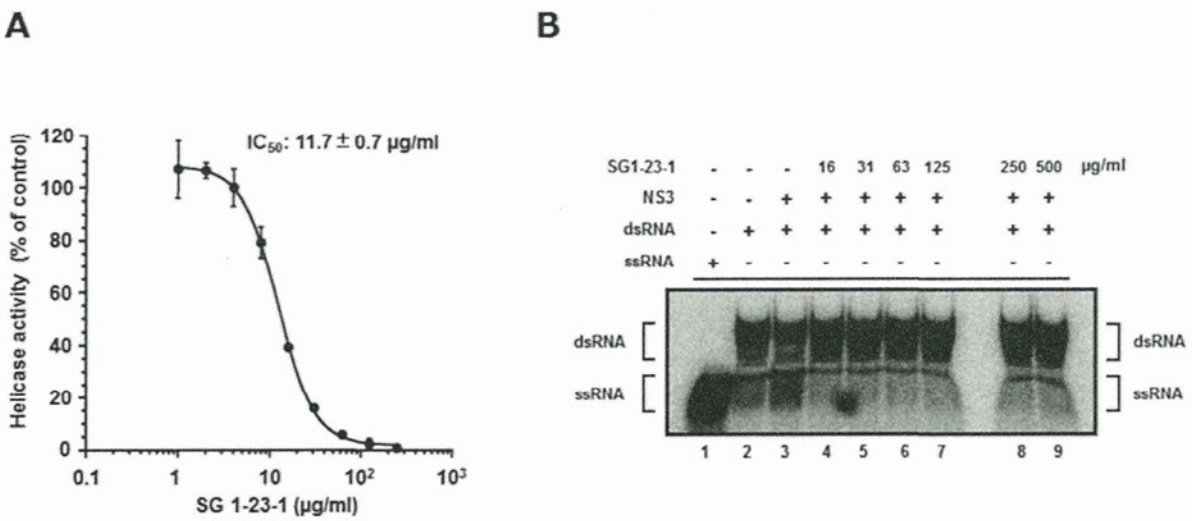

2.2. Effect of SG1-23-1 on HCV NS3 ATPase and RNA Binding Activities

The unwinding ability of HCV helicase is dependent on ATP binding, ATP hydrolysis, and RNA binding [8,9]. We examined the effect of SG1-23-1 on the ATPase activity of NS3 helicase. The ratio of free phosphate (^{32}P-Pi) in ATP (^{32}P-ATP) was measured in the presence of SG1-23-1. The reaction